Christina Huber, BSc

Improved Characterization and Performance of immobilized NADH Oxidase

MASTERARBEIT

zur Erlangung des akademischen Grades
Diplom-Ingenieurin

Masterstudium Biotechnology

eingereicht an der
Technischen Universität Graz

Betreuer
Univ.-Prof. Dipl.-Ing. Dr. techn. Bernd Nidetzky
Dr. Juan Manuel Bolivar
Institut für Biotechnologie und Bioprozesstechnik

Graz, August 2020

EIDESSTATTLICHE ERKLÄRUNG

Ich erkläre an Eides statt, dass ich die vorliegende Arbeit selbstständig verfasst, andere als die angegebenen Quellen/Hilfsmittel nicht benutzt und die den benutzten Quellen wörtlich und inhaltlich entnommenen Stellen als solche kenntlich gemacht habe. Das in TUGRAZonline hochgeladene Text-dokument ist mit der vorliegenden Masterarbeit identisch.

Datum, Unterschrift

Zusammenfassung

Seit einigen Jahren werden Enzyme aufgrund ihrer Selektivität und Arbeitseffizienz in der Industrie eingesetzt. Viele interessante Reaktionen benötigen Cofaktoren wie NAD(P)H. Diese können einen sehr großen Anteil der Produktionskosten einnehmen, da sie kontinuierlich zum Prozess hinzugefügt werden müssen. Das Enzym NADH-Oxidase (NOX) von *Thermus thermophilus* ist ein potentielles Hilfsmittel, um Cofaktoren direkt im System zu recyceln. NOX konnte bereits erfolgreich immobilisiert werden, wodurch das Enzym mehrmals eingesetzt werden kann. Im Zuge dieser Arbeit charakterisieren wir die Immobilisierung von NOX und wir ermitteln Massentransferlimitierungen der Reaktion. Des Weiteren vergleichen wir die verschiedenen Materialien, Agarose und Methacrylat, und deren Einflüsse auf die katalytischen Eigenschaften des immobilisierten Enzyms. Wir zeigen ebenfalls, dass die Art des Mixens den Massentransfer erheblich beeinflusst. Durch ein kontinuierliches Rühren der Suspension während der Reaktion können Massentransferlimitierungen verringert werden, wodurch die katalytische Aktivität von NOX steigt. Zusätzlich beeinflusst die Materialbeschaffenheit den Massentransfer. Agarose besitzt hydrophile Eigenschaften, wodurch der Transfer von Cofaktoren erleichtert wird und somit die Reaktion von NOX schneller abläuft als jene von NOX immobilisiert auf Methacrylat. Um den Massentransfer zu erleichter, setzen wir eine Beschichtung aus Polyethylenimine (PEI) ein. Diese interagiert mit den Cofaktoren und erleichtert folglich den Massentransfer zum Trägermaterial. Dadurch erhöht sich die katalytische Aktivität von NOX immobilisiert sowohl auf Agarose als auch Methacrylat. Weiteres immobilisieren wir NOX in unterschiedlichen räumlichen Anordnungen, da eine homogene Immobilisierung die katalytische Aktivität steigern soll. Das Enzym kann sowohl auf der äußeren Oberfläche des Trägermaterials (heterogene Immobilisierung) als auch in den Poren des Materials (homogene Immobilisierung) immobilisiert werden. In unseren Experimenten zeigen wir, dass eine heterogene Immobilisierung effektiver in der katalytischen Aktivität als die homogene Immobilisierung ist. Zusammenfassend konnten wir die Massentransferlimitierungen verringern und wir haben die geeignete räumliche Orientierung der Enzyme am Träger ermittelt. Zu Guter Letzt haben wir zusätzlich zum NADH Konsum auch die Produktformation durch den Einsatz von gelöstem HRP in der Reaktionssuspension detektiert und beobachtet.

Abstract

Enzymes are used in industry for several years because of many advantages due to selectivity and efficiency. Many interesting redox reactions rely on the presence of NAD(P)H, which make upscaling cost-intensive due to the continuous addition of cofactors. NADH oxidase (NOX) from *Thermus thermophilus* has been considered as a potential enzyme to use as a recycling system. Previously, NOX has been successfully immobilized, which allow an enzyme reuse within the system. In this work, we discuss the immobilization of NOX further, determine mass transfer limitations and compare two different carrier material, agarose and methacrylate, with each other. It was identified how enhanced mixing could substantially improve mass transfer. Vigorous mixing enhances the mass transfer of cofactor and substrate and thus increases the catalytic activity of NOX. Further, material properties have an impact on the mass transfer as well. We show that hydrophilic characteristics of agarose are beneficial for the activity of NOX rather than methacrylate. To enhance mass transfer of cofactors, we introduced a polyethyleneimine (PEI) coating onto the carrier. The PEI interacts with cofactors and binds them reversibly onto the carrier. We could demonstrate that PEI lowers the mass transfer of cofactors and thus increases the specific activity for NOX on agarose as well as on methacrylate. Moreover, spatial distribution of the enzyme on the carrier is described as a promising method to increase overall catalytic properties. In our experiments we demonstrate that heterogeneous distribution of NOX is more efficient than homogeneous distribution. Overall, we could decrease mass transfer limitations and detect the more appropriate option of spatial distribution of NOX on the carrier. This is shown not only by observation of NADH consumption but also by detecting H_2O_2 production by incorporation of HRP into the system.

Acknowledgement

First and foremost, I want to thank Dr. Bernd Nidetzky. He gave me the opportunity to work in corporation with Universidad de Zaragoza, Spain. I am grateful for the supervision in this project.

I also want to thank Dr. Juan Manuel Bolivar and Dr. Fernando López-Gallego. Both of them supported me in every aspect during the course of my thesis and made it possible for me to go abroad and get to know another culture, country and people. I am grateful that they were always patient and gave lots of helpful advice in every aspect to grow as a scientist and also personally.

The empirical work was performed at the department Instituto de Síntesis Química y Catálisis Homogénea at Universidad de Zaragoza supported by Erasmus+.

Big thanks to Dr. Ana I. Benítez Mateos. She helped me wherever she could and she made me feel welcome in a foreign city. I am grateful her for her great supervision in the lab as well as in personal things. I am happy I got the opportunity to work with her.

I have to thank also Susana and all the other people in the lab. Susana gave me great advice, helped me wherever she could and she also always listened to me even with non-work related things. All of the people in the lab were very warm hearted, welcomed me and some of them became good friends of mine. The work without them would have not been as fun as it was. I will be always happy to meet them again and they are always welcome wherever I am.

Ich möchte mich auch bei meiner Familie bedanken. Sie haben mich über all die Zeit unglaublich unterstützt und noch viel mehr als ich es mir jemals vorstellen hätte können. Ich kann gar nicht genug sagen, wie dankbar ich für alles bin. Sie haben mich die letzten 25 Jahre immer geleitet und mich auf den Weg gebracht, auf dem ich jetzt bin, auch wenn es nicht immer einfach war. Vor allem auch Danke an Sylvia, die mir immer die ungeschminkte Wahrheit sagt.

Ich bin auch unglaublich dankbar für all meine Freunde und deren mentalen Unterstützung. Sie haben immer einen guten Ratschlag parat, egal um was es sich handelt. Ohne euch wäre mein Leben wirklich sehr trist und langweilig. Ihr seid ein Teil meiner Familie geworden und ich möchte mir ein Leben ohne euch nicht vorstellen.

Contents

List of Figures

List of Tables

List of Abbreviations

AG	Agarose beads
AG-Gx	Agarose beads with glyoxyl groups
AG-Gx-PEI	Agarose beads with glyoxyl groups coated with PEI
APS	Ammonium Persulfate
CLEA	Cross linked enzyme aggregates
CLEC	Cross linked enzyme crystals
FAD	Flavin Adenine Dinucleotide
FITC	Fluorescein isothiocyanate
HRP	Horseradish Peroxidase
IPTG	Isopropyl-β-D-thiogalactopyranoside
K_m	Michaelis Menten Constant
K_d	Dissociation Constant
LB	Luria-Bertani media
NAD^+	Nicotinamide Adenine Dinucleotide oxidised form
NADH	Nicotinamide Adenine Dinucleotide reduced form
NOX	NADH Oxidase
OD	Optical density
PEI	Polyethylenimine
PEI25	Polyethyleneimine (25 kDa)
PEI60	Polyethyleneimine (60 kDa)
PEI10^6	Polyethyleneimine (10^6 kDa)
PU	Purolite® beads with epoxy groups
PU-Gx	Purolite® beads activated with glyoxyl groups

PU-Gx-PEI	Purolite® beads activated with glyoxyl groups coated with PEI
rpm	Rounds per minute
TB	Terrific broth
TEMED	Tetramethylethylenediamide

1 Introduction

1.1 Enzyme technology and enzyme immobilization

1.1.1 Importance of immobilized enzymes

Biotransformations have been used in food and drug industry ever since and the use of isolated and immobilized enzymes has increased in the past few years. Biofuels, pharmaceuticals, fine chemicals and detergents are just a few examples of the processes done by enzymes [1]. Enzymes are very selective, which lead to an enantiopure product. Furthermore, enzymes are very efficient under mild conditions. In comparison to chemical synthesis, no harsh conditions such as extreme temperature or addition of harmful chemicals are needed in enzyme technology. Therefore, enzymes are less energy consuming and more sustainable. These features make enzymes a promising tool in a variety of processes which were done chemically in the past [2]–[4]. Nevertheless, there are some disadvantages that have to be overcome in applied biocatalysis. Enzymes are unstable due to different inactivation conditions and have a short durability [2].

Immobilization helps to overcome these issues and enhances stability and further on increases the production yield. Moreover, immobilization allows the reuse of the enzyme and facilitate the separation of the product from the reaction system [2], [3], [5]. For industrial application it can be considered to use a continuous reactor which enables the reuse of the immobilized catalyst [6]. This can be advantageous because otherwise enzymes would be lixiviated as the products are harvested and purified. Immobilization enables the reuse of the enzyme for several rounds and this leads to an even higher production yield [2]–[4].

1.1.2 Types of immobilization

There are 3 main options to immobilize enzymes: binding on carrier, entrapment and cross-linking. Entrapment defines the immobilization of enzymes by building a polymeric structure around the enzyme. Polyacrylamide and silica sol-gels are used for this method. The polymeric structure is synthesized in presence of the enzyme [2], [7]. Cross-linking are enzyme aggregates or crystals which stay functional even after aggregation. The advantage of this method is that no support is required. This means that the whole aggregate consists out of concentrated enzyme. It is proven that such CLEAs (cross-linked enzyme aggregates) have a high stability and the production cost

is low. Nevertheless, CLEAs have some disadvantages due to their mass transfer limitations and low stability [8], [9]. Cross-linking is an irreversible immobilization method [10]. Contrastingly, immobilization of enzymes on carriers can be reversible as well as irreversible depending on the way of enzyme-carrier interaction [2], [3].

The most used immobilization method is binding to pre-existing carrier. Therefore, enzymes are bound onto a support which might help to increase the stability dramatically. These carriers can consist out of a variety of materials, like inorganic, synthetic organic polymers and natural polymers [2], [5]. Most prominent examples are glass or ceramics (inorganic materials), acrylic resins like Eupergit C (organic polymers) and starch, agarose and cellulose (natural polymers). These are mainly water-insoluble and therefore they are suitable for enzyme immobilization [2], [11], [12].

1.1.3 Binding interactions of enzyme and carrier

Enzymes can be immobilized onto the carrier through reversible and irreversible chemistries. Hydrophobic and ionic interactions, hydrogen bonds and affinity are reversible bindings. On the one hand, these bonds have the disadvantage of promoting the enzyme leaking during the usage. Mostly environmental conditions can influence leaking by ionic strength, solvents or pH [3], [10]. On the other hand, the advantage of this technique is that the enzyme can be desorbed from the carrier, and the carrier can be reused after the activity of the enzyme decreases. This leads to a more sustainable use of carrier which are mostly very pricy. Irreversible bindings overcome the lixiviation problem because the enzymes are fixed onto the carrier. Such bindings are usually covalent bonds. One negative issue is that the carrier cannot be reused after the enzyme got inactivated. Nevertheless, the irreversible binding is very convenient as it increases the durability and stability of the enzyme. The different binding methods can be classified into 3 categories [3]:

- Physical adsorption

To start with, physical adsorption is an easy way to immobilize enzymes onto a carrier. Therefore, the natural properties of the proteins are used to bind it onto the suitable material. Physical adsorption can be subdivided into hydrophobic interactions, ionic interactions and hydrogen bonds. Some enzymes as for example lipases have hydrophobic residues on their surface. This can be used to bind these enzymes on lipophilic carriers [3].

Immobilization by ionic interactions has the same strategy as ion exchangers. The interactions of both enzyme and carrier depend on the negative and positive charged surfaces as they are attracted to each other. Therefore, the natural charge of the enzyme has to be known to modify the surface of the carrier to the complementary charge. Nevertheless, ionic interactions are very weak and can be disrupted in presence of high pH or ionic strength. Another aspect to consider is that highly charged supports may lead to side effects. These could interfere with the substrate or the product [3], [13]. Under optimized conditions ionic interactions can be a useful and simple tool to immobilize enzymes onto a carrier. Furthermore, the carrier can be reused after enzyme inactivation because of the reversible interactions [10].

- Covalent binding:

In aqueous media covalent bonds are preferred [3]. Therefore, amino and other functional groups (sugar residues) can be used to attach the enzyme to the carrier. The side chains of amino acids, for example Lys, Cys, His, Tyr, interacts as a nucleophile to attack chemical residues of the carrier. Covalent binding can be reversible as well as irreversible. The reversible interactions are imine or disulfide bonds. These bonds can be transformed into irreversible ones applying mild reducing agents, resulting in secondary amine and thioether bonds, respectively. Covalent interactions are very strong bonds but usually the orientation of the enzyme on the carrier is arbitrary. Nevertheless, these bindings enhance stability and durability of the enzyme even though the carrier cannot be reused after inactivation of the enzyme [14]–[17].

- Affinity:

Affinity properties are widely used in chromatography. Nonetheless, the same principles are used in immobilization. It relies on biomolecular interactions and selectivity. Antibody and antigen-, avidin and biotin-, his-tag and metal ion interactions are just a few examples of affinity bonds. This method requires modifications on the enzyme and surface of the carrier to achieve a proper binding. As the orientation of the enzyme can be controlled, the enzymatic activity is high. Although the binding with affinity is quite stable under certain conditions, lixiviation may occur as this binding is reversible [18], [19].

1.1.4 Spatial localization on carrier

Carrier material can have a non-porous as well as a porous structure. Porous structures can be very beneficial as a higher amount of enzyme can be immobilized onto the carrier [18, p. 706], [20], [21]. Enzymes can be immobilized on the outer surface (heterogeneous) as well as in the channels of the carrier (homogeneous) as shown in **Figure 1**.

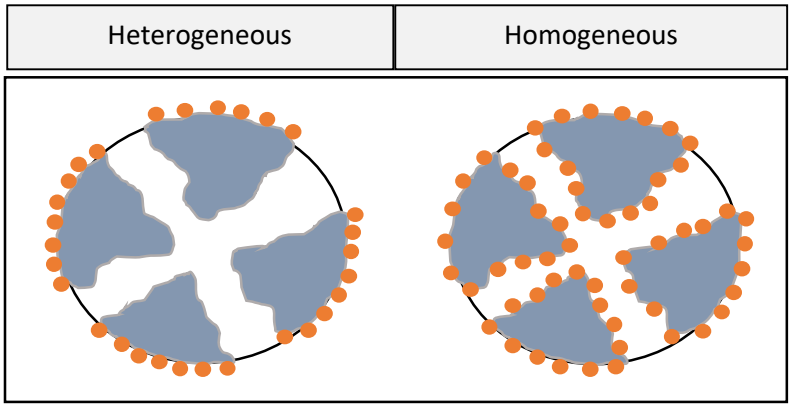

Figure 1 Enzyme distribution on a porous carrier. *The enzyme can be located on the outer surface of the carrier (heterogeneous) or in the pores of the carrier (homogeneous).*

The increase of enzyme loading by homogeneous distribution on to the carrier is promising in increasing catalytic efficiency. Nevertheless, homogeneous distribution faces a variety of issues to fully utilize the immobilized enzymes like substrate diffusion. Hitherto, several publications describe the limitations of mass transfer in heterogeneous catalysts and porous carrier material [22]–[24].

1.2 Mass transfer of heterogeneous biocatalysis

In immobilized enzymes, the reaction rate is affected by processes of mass transfer. In enzyme immobilized in porous particles, there is a step of external mass transfer towards the solid surface, and a second step of internal mass transfer [18, p. 707].

1.2.1 Outer mass transfer

In solution, enzymes and substrates are homogenously distributed in the liquid and the enzymes can react rapidly with the substrate available. As enzymes are immobilized onto a solid carrier, the reaction depends also on the mass transfer. A boundary layer surrounds the carrier and the immobilized enzymes. This means, a concentration gradient of the substrate is build up between the solution and the solid carrier. As the enzymes consume the substrate, the substrate has to overcome the boundary layer and diffuse to the enzyme from the actual solution. On the one hand, if the reaction rate is high the reaction is limited by the substrate. In other words, the

substrate gets faster consumed than the substrate diffusion affects to the enzyme. On the other hand, if the reaction rate is slow the mass transfer corresponds to the reaction rate and the mass transfer does not limit the reaction [18, pp. 707–709].

1.2.2 Internal mass transfer

In enzymes immobilized in porous carriers (section 1.3), internal mass transfer has also an impact on the catalytic efficiency of the enzyme. Internal mass transfer is defined as the transfer of a molecule from the surface of the particle into the inner part. It has to be considered that the substrate could be consumed by the enzymes located in the outer phase even before the substrate is diffused into the inner phase of the carrier. That means that the mass transfer has to be rapid enough to negligibly affect the reaction rate of the catalyst [18, pp. 707–709]. Nonetheless, the consumption of the substrate leads to a continuous concentration difference between the outer and the inner milieu. This enables a constant mass transfer from the bulk solution into the carrier [21], [25], [26]. The efficiency of the transport depends on the carrier properties, like charge, pore size and hydrophobicity. Further on, the mass transfer coefficient depends on viscosity, density and diffusivity of the reaction solution [18, pp. 707, 739–740]. As described elsewhere, a milieu is build up within the particle [21]. This milieu of the inner particle has different properties, not just the particle properties but also the potential difference in pH. The enzymes influence the surrounding conditions by the catalyzed reaction which leads to different concentrations of substrate and product between the particle and the reaction solution [21], [25], [27]. All of these parameters have an impact on the mass transfer and thus can be adjusted to decrease mass transfer limitations [18, p. 744].

1.2.3 Overcoming mass transfer limitations

As described in the sections above, mass transfer has a crucial impact on the catalytic activity on the immobilized enzyme. Outer mass transfer can be overcome by altering mixing conditions, different reactor types, e.g. spinning basket reactor, which increase fluid velocity, increasing substrate concentrations and reducing the size of the particle. Internal mass transfer effects can be minimized by catalyst engineering to reduce the reaction rate, increasing diffusivity effect and increasing the substrate concentration on the surface of the particle. Nevertheless, decreasing the reaction rate is not always beneficial for the overall reaction [18, pp. 744–745].

1.2.4 Spatial localization of enzymes as tool to minimize mass transfer resistances

As discussed in section 1.4, the control of enzyme distribution might be important to improve the enzyme activity. Spatial distribution of enzymes allows a higher enzyme loading on the carrier and thus the catalytic performance should increase [18, p. 706], [20], [21]. Especially multi-enzyme systems can benefit from the co-localization on porous carrier as discussed in recent publications [27], [28]. In multi-enzyme systems the inner milieu is used to enhance the transfer of one product to the next enzyme which uses the product as a substrate. The co-immobilization on the same carrier facilitate a near localization to mitigate the transfer of product and substrate. This increases the overall catalytic efficiency of the enzymes. These cascades are less limited by mass transfer which promotes multi-enzyme systems on the same carrier to be a promising tool in applied biocatalysis [27]–[29]. As described elsewhere, this system can be used for example to recycle cofactors in-situ in the carrier [29].

1.3 NADH oxidase as a recycling system

A number of interesting redox reactions rely on the use of NAD(P)H based cofactors. From a practical point of view, the cofactor has to be used in small amounts and they should be recycled within the same system. Most often, cofactors are continuously added into the reaction system which take up a big part in the production cost. A promising solution could be a cofactor recycling system [30]. By implementation of another enzyme which recycle redox cofactors, the amount of cofactors externally needed can be reduced or even avoided and thus production costs can be decreased. Nonetheless, such enzyme cascades need to be adjusted to each other. Every enzyme has its special optimal surrounding conditions concerning pH, ionic strength and temperature. Meaning, compromises have to be made in order to successfully apply a multi-enzymatic-system [31], [32].

One potential recycling system could be NADH oxidase (NOX). NOX converts NADH into NAD^+ and it is part of the respiratory chain in nature [33], [34]. On the one hand, there is NOX converting NADH into NAD^+ producing H_2O. On the other hand, there is another type which produces NAD^+ with H_2O_2 as a byproduct (**Figure 2**) [35].

Figure 2 Reaction mechanism of NOX from Thermus thermophilus. *NOX catalyzes the reaction from NADH to NAD*. FAD changes from the oxidized (ox) to the reduced (red) form which is further changed from the reduced to the oxidized form by producing H_2O_2 from O_2* [37].

The enzyme of our interest belongs to the second type of NOX and origins from *Thermus thermophilus* HB27. This gram-negative bacterium exists under extreme temperature conditions in hot springs and industrial compost. Its temperature range is between 50°C and 82°C [36]. Thermophilic enzymes are useful because they can resist a broad range of temperature and can be easily purified from the other enzymes expressed in the host cell. NOX is a flavoenzyme and one unit of the homodimer has a size of about 27 kDa. The advantage of the enzyme is the high stability against a broad range of pH and temperature which enables the immobilization under alkaline conditions. The optimum temperature is around 70°C but the specific activity remains quite high (37 U/g) also under lower temperatures of 37°C [33], [37]. This allows the implementation of this enzyme as a recycling system coupled with other enzymes with lower optimal temperature.

NOX uses two different cofactors, FAD and NADH. FAD is intrinsically bound to the enzyme. It has been shown that NOX has a certain activity even without FAD. Nevertheless, a small addition of exogenous FAD increases its catalytic efficiency. On the other hand, NADH is consumed within the reaction and NAD^+ is produced. This is advantageous because NOX can be used as a recycling system for NAD^+ during oxidation reactions [33], [35]. NAD(H) belongs to the group of nicotinamide cofactors. As redox reactions become more popular in biotransformation these days, the implementation of easy and efficient recycling systems is very much in demand [30]. Therefore, the characterization and research of immobilized NOX is crucial.

1.3.1 Oxygen as a substrate

NOX uses oxygen as an electron acceptor to oxidize NADH into NAD^+ and H_2O_2 [35]. The advantage of oxygen as electron acceptor is that it is naturally occurring. Therefore, it is cheap and neither non-toxic nor influencing the majority of other reactions [38]. Although O_2 is in solution in open vessels, its solubility depends on temperature and pressure in the gas phase [18, pp. 409–410]. At room temperature

(25 °C), the oxygen concentration in aqueous solutions is around 0.25 mM. In oxygen consuming reactions, this can be a limiting factor. However, oxygen available in the reaction system also depends on the mass transfer between the liquid and the gas interface [39]. The mass transfer of oxygen from the gas phase into the liquid is comparable to the solid-liquid mass transfer described above in section 2. A boundary layer with film resistance of both sides of the phases influences the oxygen transfer from the gas into the liquid phase. Oxygen has to overcome thus both films, respectively, to change from one phase into the other. The concentration difference is the driving force for the oxygen transfer from the gas phase into the liquid phase. For immobilized enzymes, two more barriers for the oxygen transfer have to be overcome, the external as well as the internal solid-liquid mass transfer. As oxygen is consumed within the reaction of NOX, the concentration difference is constantly pushing forward the mass transfer, which is explained in more detail in section 2 [18, pp. 383–393].

As the gas-liquid-mass-transfer can be limiting in a resting system, several aeration methods are developed to overcome external oxygen limitations. In small scale, the surface aeration could be sufficient enough to provide oxygen for the reaction. Therefore, the reaction mixture is mixed and the upper surface is thus expanded a bit more for a better mass transfer [18, p. 429]. In large scale, the most common method is bubble aeration. Therefore, gas bubbles are introduced into the reactor to provide a homogeneous aeration in the solution. It has to be considered, that the bubbles should be small so the surface of the boundary layer is as large as possible to increase the oxygen supply. The downside of bubble aeration is that enzymes are very sensitive to the shear forces of the gas bubbles [40], [41]. As the enzymes get in contact with the boundary layer of the gas-liquid interface, the enzyme gets damaged. This can negatively affect the activity and productivity of the enzyme. Another way is membrane aeration. This is a much more sensitive method to ensure oxygen supply in the reactor. Therefore, gas is immersed into the suspension by silicone or microporous polypropylene. Oxygen diffuses through the walls into the solution without bubble forming [18], [42], [43]. Nonetheless, aeration systems mitigate only external diffusion restrictions. In heterogeneous systems, as immobilized enzymes, internal diffusion restrictions have to be overcome by different approaches like protein engineering, tuning particle- and pore size and also the distribution of the enzyme within the carrier [18, pp. 744–745].

The aim of this master thesis is to improve the activity of NOX by controlling the immobilization of the enzyme in porous particles. With that we aim to accomplish two sub-objectives. First, we wanted to improve the mass transfer of oxygen into the porous carriers through controlling the spatial distribution of the carriers and the mixing. To this aim, we immobilized NOX heterogeneously and homogenously onto agarose as well as purolite (methacrylic matrix). Activity of both enzyme preparations were observed under different mixing conditions to mitigate mass transfer limitations. Secondly, we aimed to solve the mass transport limitation of NADH by co-immobilizing cofactors and the enzyme within the same porous structure. To do so, we coated both carrier preparations (homogenous and heterogeneous immobilized NOX) with a cationic polymer (PEI). PEI has the ability to bind NADH as well as FAD and thus mass transfer limitations can be mitigated. The activity of the enzyme preparations was observed under different mixing conditions and the impact of PEI onto the mass transfer was detected.

2 Materials and Methods

2.1 Materials

Chemicals and other substances such as hydroxylamine, ethanolamine, ethanol, glycerol, bicarbonate, potassium iodide, sodium borohydride, sulfuric acid, avidin (from egg white), Rhodamine B isothiocyanate, FITC, tryptone, yeast extract, glycerol, sodium chloride, potassium phosphate monobasic, potassium phosphate dibasic, monosodium phosphate, disodium phosphate, Ampliflu™ Red, HRP, PEI with 25, 60 and 10^6 kDa and ampicillin are purchased from Sigma Aldrich. IPTG and NADH are from Gerbu Biotechnik GmbH. FAD^+ and bovine serum albumin is acquired from Cymit quimica. Agarose – 2% BCL Agarose Bead Standard (50-150 µM) is purchased from Agarose Bead Technologies and Purolite® - ECR8204 F is from LifeTech. The Bradford assay is purchased from BIORAD.

The bacterial strain used in this thesis is *Escherichia coli* BL21 containing the plasmid *nox*_pET22a.

The equipment is acquired as listed:

Equipment	**Use**	**Company/Product description**
Mini Bio-Spin® Chromatography Columns	Protein labelling	BIO-RAD
Microplate reader Epoch 2	Determination of activity assay, protein concentration, cell density	BioTek®, software Gen5
Microplates Standard 96		Biogen
Spectrophotometer		Unicam UV4-100 double beam UV-visible spectrophotometer
External magnetic stirrer		Thermo Scientific – CIMATECi Telemodul
pH meter		Crison GLP22 pH ISE
Sonicator	Purification	Sonoplus Serie 4200, Banelin

Centrifuge		GUSTO® High-speed mini centrifuge
Laminar flow hood		Cruma 870FL
Confocal Microscope	Protein distribution on carrier	ZEISS LSM 880
SDS-PAGE electrophoresis (chamber, buffer, staining and destaining solution, gel components)	Protein concentration, -composition	Mini-protean Tetra System, BIO-RAD
Optical Oxygen Meter – FireStingO_2	Oxygen consumption	Pyroscience

The media for protein expression is prepared as listed. The media is mixed till the solution is clear. Afterwards, it is autoclaved to provide a sterile environment for cell cultivation. It is important to sterilize the potassium phosphate solution before adding to the sterile TB media.

Media	**Composition**
LB	Tryptone – 10 g/L Yeast extract – 5 g/L NaCl – 5 g/L Fill up with water till 1 L
TB	Tryptone – 12 g/L Yeast Extract – 24 g/L Glycerol – 4 mL Water – 900 mL Autoclaving After cooling 100 mL of: KH_2PO_4 – 0.17 M K_2HPO_4 – 0.72 M

2.2 Methods

2.2.1 Growing and expression conditions

A glycerol stock of *E. coli* BL21 carrying the plasmid *nox*_pET22a was provided by Fernando López-Gallego´s group. The plasmid harbours the gene encoding the NADH oxidase from *T. thermophilus* HB27 and is expressed under the control of the T7 promoter induced by IPTG. Using this glycerol stock, an overnight culture in 3 to 5 mL LB media and 30-50 μg/mL of ampicillin is prepared. This is incubated under orbital shaking at 37°C [33], [44].

Afterwards, the cells are cultivated in LB or TB media containing 50 μg/mL of ampicillin. In 50 mL of media containing the antibiotic, 1 mL of overnight culture is added. The flasks are incubated under orbital shaking at 37°C until an OD of 0.4 to 0.6 is reached. The OD is measured photometrically at an absorbance of 600 nm by taking 350 µL of growing cell culture and the same amount of sterile media as a reference. As *nox*_pET22a carries a T7 promotor, the cells are induced by adding 1 mM IPTG. The expression is performed under orbital shaking and 37°C for 3 to 4 hours [33].

For cell harvesting, the suspension is centrifuged at 4,000 rpm for around 20 minutes. The media gets discarded and the cell pellets are frozen at -20°C for further uses [33].

2.2.2 Cell disruption and purification

The pellets of the expression are resuspended in 25 mM sodium phosphate buffer at pH 7. Afterwards, the cells are disrupted using sonication (5 sec ON, 5 sec OFF, 40% amplitude) for 20 minutes. The disrupted cells are centrifuged at 10,000 rpm for 20 minutes to remove the parts of the cell wall and other non-soluble components from the soluble proteins. Therefore, the supernatant is carefully transferred into new tubes for further purification steps.

As mentioned previously, NOX has a temperature optimum at 70°C [45]. This feature is used to purify the enzyme by thermoprecipitation. To do so, the supernatant is incubated in a water bath at 80°C for 45 minutes. Proteins of *E. coli* are not stable to withstand this temperature and precipitate. Afterwards, the suspension is centrifuged at 10,000 rpm for further 20 minutes. The remaining solution contains the pure NOX [33].

To analyze the protein content, aliquots of each disruption and purification step are taken. The first aliquot is taken right after sonication as cell lysate. In this sample all

soluble and insoluble cell components are contained. The second aliquot is taken after centrifugation. This solution contains all soluble proteins. The last aliquot was taken after the heat treatment and centrifugation. In this solution, pure NOX should be remained.

2.2.3 SDS gel electrophoresis

The SDS-PAGE is done as described in the product manuals of BIO-RAD. For the SDS gel electrophoresis, a gel with two different densities is prepared. First of all, the lower gel, the resolving gel, has a density of 12%. This part separates the proteins from each other. The gel is prepared as followed, which provides 4 gels in total:

- 6.8 mL of distilled water
- 8 mL of bisacrylamide (30%)
- 5 mL of resolving buffer
- 0.2 mL of SDS (10%)
- 0.2 mL of APS (10%)
- 0.02 mL of TEMED

All of the ingredients are mixed with each other. TEMED should be added at the end as it starts the polymerization reaction. As soon as TEMED is added, the solution is divided on the 4 gel frames. Additional isopropanol on top of the gel helps to the gels homogenously flat. After about 30 minutes the gels are solid. Afterwards, the isopropanol is removed. The second upper gel is the stacking gel with 4% of density. This part of the gel collects the samples on one line before proteins get separated, which is prepared as followed:

- 6.1 mL of distilled water
- 1.3 mL of bisacrylamide (30%)
- 2.5 mL of stacking buffer
- 0.1 mL of SDS (10%)
- 0.1 mL of APS (10%)
- 0.01 mL of TEMED

As for the resolving gel, TEMED is added at the end and the solution is transferred on the four gel frames. On top of the gel, a comb is positioned. The comb helps to form the sample slots. After another 30 minutes the gel should be solid. The gel is stored in wet paper towels and aluminium foil till its final use.

For the gel electrophoresis, the comb is removed from the gel. The gel is put into the chamber which is filled with tris-glycine-buffer for the appropriate amount of gels used in the electrophoresis. The tris-glycine-buffer is a 10x premixed electrophoresis buffer at pH 8.3, which contains 25 mM tris, 192 mM glycine and 0.1% SDS. For usage it is diluted to a 1x buffer using distilled water. The gel is acclimatized in the chamber with the buffer. In the meantime, the samples are mixed with Laemmli buffer [46] in a dilution of 1:1 to stain the protein samples. A total volume of 10 to 30 µL should be used. This solution is incubated at 100°C for at least 5 minutes. Afterwards, 5 to 10 µL of the samples are transferred into each well of the gel. Preferably at the first or last well of the gel, 5 µL of an adequate standard as a reference to the unknown samples are transferred as well. The lid with the electrodes is put onto the chamber to close and connect the electric circuit. At the beginning, 100 V is set to concentrate the samples in the stacking gel. Afterwards, 150 V is used to perform the actual electrophoresis. The electrophoresis runs till the proteins reach about 1 cm above the end of the gel.

After gel electrophoresis, the gel is carefully separated from the frame and washed with distilled water. To make the proteins visible, the gel is transferred into a little container filled with a staining solution (commercially available Coomassie Brilliant Blue R-250 Staining Solution from BIO-RAD) until the gel is covered up with the solution. This is incubated for at least 30 min. Afterwards, the staining solution is removed and a destaining solution (40% methanol, 50% distilled water and 10% acetic acid) is put into the container with the gel. This is incubated for another hour till the gel is clear. At the end, the gel can be transferred onto a white surface to have the best contrast for observation of the separated proteins [47].

2.2.4 Measurement of protein concentration

The BIO-RAD Bradford assay is a fast method to determine the protein concentration in a solution. This assay is done as described in the product manuals of the company BIO-RAD [48], [49]. The BIO-RAD Bradford stock solution must be diluted 5 times with distilled water. For the standard curve different concentrations of albumin diluted in distilled water is prepared. Therefore, 1 mg/g, 0.5 mg/g, 0.25 mg/g, 0.125 mg/g and 0.0625 mg/mL of the albumin solution are prepared. If the unknown concentration of protein solution is meant to be quite high, it can be diluted with water. This method was adapted for a 96-wel plate reader. In each well, 200 µL of diluted Bradford solution are

mixed and 5 µL of each standard concentration and of the samples are added. This is incubated for 5 minutes and the absorbance is measured at 595 nm.

As we also worked with very low enzyme concentrations, another standard curve is prepared. This is performed with 0.125 mg/mL, 0.0625 mg/mL, 0.03125 mg/mL, 0.0156 mg/mL and 0.0078 mg/mL of albumin solution. For such low concentrations, 150 µL of Bradford solution and 50 µL of standard or sample were mixed into the well. This is also incubated for 5 minutes before the absorbance at 595 nm is measured [50].

The absorbance of each standard concentration can be plotted against each other. The relation between the absorbance and the standard is linear. This linear equation is used to calculate the unknown concentration of the enzyme solution [50].

2.2.5 Activity assays

2.2.5.1 Activity assay by NADH monitoring

The activity of the NOX was measured by monitoring the initial reaction rate of NADH oxidation. Spectrophotometric detection (340 nm) is used for quantification of NADH. We measured the NADH concentration in two different ways, microplate reader and spectrophotometer. In the microplate reader, the suspension of the reaction was mixed by orbital shaking, which mixes the reaction shortly right before measuring. The spectrophotometer uses external, magnetic stirring in the cuvette to mix the reaction suspension. This allows a continuous and constant mixing with the whole reaction.

The reaction set-up us described as follows for both, microplate reader and spectrophotometer. The reaction mix contains 0.2 mM NADH and 0.15 mM FAD^+ dissolved in 25 mM sodium phosphate buffer at pH 7 [33], [44]. 5 mL of reaction mix were prepared as stock. For the soluble enzyme, the enzyme solution was diluted 10 times in sodium phosphate buffer at pH 7. 5 µL of the diluted enzyme is added into the well. The reaction is then triggered by adding the reaction mix before starting the measurement at an absorbance of 340 nm and at 25° C [33], [44]. Using the spectrophotometer and magnetic stirring, 1.5 to 2 mL of reaction solution are transferred into a cuvette. The reaction is triggered by adding the enzyme. 10 µL of the soluble enzyme is added to the reaction mixture. If the reaction is too fast, the soluble enzyme can be diluted. Parallel to the reaction, also a blank containing the reaction solution without the enzyme is measured. The samples are measured in triplicates.

The slope determines the NADH concentration in A/min (Δ). The volumetric activity (U/mL) can be calculated using **Equation 1**.

Equation 1 Determination of activity (U/mL) using the slope of the NADH absorbance over time. *Δ determines the absorbance of NADH over time (A/min), V_{total} is the total reaction volume (mL), ε is the molar extinction coefficient (NADH: 6.22 $mM^{-1}*cm^{-1}$), d is the path length of the cuvette (1 cm) and v_{NOX} is the volume of enzyme solution (mL). If necessary, the dilution factor should be incorporated.*

$$U/_{mL} = \frac{\Delta * V_{total}}{\varepsilon * d * v_{NOX}}$$

The specific activity (U/mg) of soluble NOX can be calculated by multiplying the volumetric activity with the protein concentration: U/mL*c(mg/mL).

2.2.5.2 Immobilized NOX

For immobilized NOX, the same procedure was done. Main modifications are mentioned as followed. As the immobilized NOX is in a suspension, a suspension factor of 10 is used in most cases. Further on, the amount of enzyme was adjusted if the reaction rate is too low. Next, in the microplate reader, 10 µL of suspension is transferred into the well. For the photometer, between 50 µL and 150 µL of suspension are taken depending on the immobilized NOX on the carrier. It is important that the ratio between suspension and total reaction volume is not higher than 1 to 10.

2.2.5.3 Activity assay by oxygen sensing

Another way to measure the activity of NOX is to measure the oxygen consumption. This is done by monitoring the decrease of oxygen during the reaction using an oxygen sensor from Pyroscience (Optical Oxygen Meter – FireStingO_2). The initial reaction rate and thus the volumetric activity (U/mL) can be calculated using the initial slope of oxygen consumption (µmol/L per minute).

For the set-up, a 4 mL glass beaker is used. The reaction is mixed using magnetic stirring at 300 rpm and the reaction takes place at 25°C and 25 mM of sodium phosphate buffer at pH 7.0 at the indicated concentration of NADH [25], [33], [43].

The reaction conditions are based on the experiments described by Rocha-Martín *et al*., 2011 [33]. Modifications to this protocol are done as followed. The total reaction volume was 4.1 mL containing 400 µL of carrier suspended in a 1 to 10 ratio in the same buffer described above. The carrier is added to the buffer and the oxygen sensing is started. Afterwards, FAD (final concentration of FAD: 0.13 mM) is added. The reaction is initiated by adding NADH into the glass beaker. The final concentration of NADH in the reaction varied (0.2 mM and 3 mM) for the experiments.

2.2.5.4 Activity assay for detection of H_2O_2 using HRP

For this reaction solution, the same concentrations of cofactors and experimental conditions are used as previously described. Additionally, we modified the reaction mix by adding 25 µg/mL of HRP and Ampliflu™ Red up to 0.05 mM. Except for the sample with immobilized NADH, where there is no NADH in the reaction mixture as the NADH is already bound onto the carrier. The reaction is observed at 340 nm for NADH consumption and additionally, the reaction of Ampliflu™ Red is observed at 520 nm [51]. This can be done simultaneously using the microplate reader.

2.2.5.5 Study of the activity dependency on the cofactor concentration: Determination of K_m of NADH

The activity of the immobilized NOX is measured at different NADH concentration. This allows the determination of the kinetic parameters of NADH. To do so, an immobilized enzyme containing 1 mg/g NOX is used and different concentrations of NADH are used starting with 0.1 mM NADH till 4 mM NADH. The conditions of the measurements stay the same under orbital shaking using 0.15 mM FAD^+ and 25 mM sodium phosphate buffer at pH 7. As the photometer has limitations of measuring absorbance of high concentration of, in this case, NADH, an indirect method is used to determine the K_m. Therefore, the reaction is set up in a syringe using a total reaction volume of 3.1 mL. The reaction is triggered by adding 100 µL of the immobilized enzyme into the reaction mixture and it is mixed under orbital shaking. Approximately 200 µL samples of the supernatant are taken after 0, 4, 8 and 12 minutes. As the supernatant is removed from the immobilized enzyme, the reaction stops. Afterwards, the samples of each time point are diluted and the NADH concentration of each sample is measured photometrically in the microplate reader at 340 nm. The linear decrease of NADH concentration is taken to calculate the specific activity.

The specific activity is plotted against the NADH concentration. The K_m and V_{max} are calculated by a non-linear regression by using Origin using **Equation 2** [18].

Equation 2 Michaelis Menten equation. *v is the reaction rate and V_{max} the maximal achievable reaction rate. S stands for the substrate concentration and K_m determines the substrate concentration at half of V_{max}.*

$$v = \frac{V_{max} * S}{K_m + S}$$

2.2.6 Enzyme immobilization

2.2.6.1 Preparation of carriers for enzyme immobilization.

Agarose is activated with glyceryl groups as described elsewhere [52]. Commercially available Purolite (ECR8204F) is activated with glyoxyl groups. To do so, the carrier has to be hydrolysed first as following reported procedures. Purolite display surface epoxy groups as reactive groups. They are hydrolysed to glyceryl groups by sulfuric acid. Therefore, per 1 part, carrier 10 parts of solution are used. To start with, the carrier is incubated with 100 mM H_2SO_4 overnight. Afterwards, the sulfuric acid is removed and the carrier is thoroughly washed with distilled water. Further, activation of the both carriers, agarose and Purolite, with glyoxyl was carried out by oxidation using 30 mM $NaIO_4$ for further 2 hours. After incubation, the $NaIO_4$ is removed and the carrier is thoroughly washed once again with distilled water. The reagent oxidizes the glyceryl groups to glyoxyl [44], [53].

2.2.6.2 Quantification of aldehyde groups

The aldehyde groups are quantified as followed. 100 mg of carrier are added to 1 mL of 30 mM sodium periodate. The suspension is incubated for 1 h under shaking. Then, 100 µL of the supernatant are taken and mixed with 1 mL of KI (10% (p/v)) in distilled water and 1 mL of saturated sodium bicarbonate pH 8.5. As a blank, 100 µL of distilled water are mixed with 10 % KI and saturated sodium bicarbonate. The same procedure is followed for the initial $NaIO_4$ solution. Afterwards, the solutions are measured photometrically at 405 nm. The absorbance of the initial solution and the supernatant after incubation with the carrier are taken to calculate the amount of aldehyde groups per g carrier [53].

2.2.6.3 Enzyme Immobilization (Purolite and Agarose)

Both carriers, PU-Gx as well as AG-Gx can be used in the same way for immobilization. The carrier is pre-washed with 100 mM sodium bicarbonate buffer at pH 10. Afterwards, 100 mM sodium bicarbonate buffer and the specific amount of enzyme are mixed. If necessary, the pH is set because the immobilization is dependent on the high pH of the solution. Per g of carrier, 10 mL of enzyme solution is added and the suspension is incubated under orbital shaking for 3 hours. To make sure NOX is fully immobilized, a sample of supernatant is withdrawn after 3 hours and the specific activity is compared with the blank solution, which contains the reaction solution with the same amount of enzyme not incubated with the carrier. If the immobilization is not

complete yet, the incubation time is increased. Afterwards, 1 mg/mL of sodium borohydride is added to the suspension and it is incubated for 30 minutes. This reducing step binds the enzyme irreversibly on the carrier. Finally, the carrier is washed at least 3 times with 25 mM sodium phosphate buffer at pH 7. This process without containing any other additives achieves a heterogeneous, fast, immobilization [33].

For homogeneous, slow, immobilization, three different variations are done. First of all, the enzyme solution is prepared as described above, but adding either 10 or 100 mM of ethanolamine to the sodium bicarbonate buffer. The second variation is proven for AG-Gx and contains 10 mM of hydroxylamine [44]. This is also tried for PU-Gx. Purolite is made out of polyacrylate, which is more hydrophobic [54]. In order to avoid hydrophobic interactions between the enzyme and the carrier, a third variation is performed by adding 10 mM hydroxylamine and 30 % (v/v) ethanol to the sodium bicarbonate buffer [55]. All of those variations are incubated overnight. According to the protocol described above, the protein concentration in the supernatant is frequently determined to achieve the best immobilization yield. Afterwards, the carrier is reduced with 1 mg/mL sodium borohydride for 30 minutes. Finally, the carrier is washed several times with 25 mM sodium phosphate buffer at pH 7 [33].

2.2.6.4 Parameters of immobilization and activity

For every immobilization process, following parameters have to be determined.

- Protein load:
  The protein load determines the mg of NOX immobilized per g of carrier (mg/g) [44].
- Immobilization yield:
  The immobilization yield is the final amount of NOX immobilized on the carrier in %. Therefore, the protein concentration of the starting solution and from the supernatant after immobilization is measured with the Bradford assay. The yield is calculated using **Equation 3**:

Equation 3 Immobilization yield (%). *Protein concentration after immobilization ($c_{after\ immobilization}$) is divided by the starting protein concentration ($c_{before\ immobilization}$) and multiplied by 100 to receive the percentage. This number has to be substituted by 100 to get the percentage of NOX bound on the carrier.*

$$Y(\%) = 100 - (\frac{c_{enzyme\ supernatant}\left({}^{mg}/_{mL}\right)}{c_{offered\ enzyme}\left({}^{mg}/_{mL}\right)} * 100)$$

- Specific activity:

  The specific activity determines the enzymatic activity per mg of enzyme. The calculation can be described as following (**Equation 4**):

Equation 4 Specific activity (U/mg) of soluble (a) and immobilized (b) enzyme*; For the soluble enzyme, the volumetric activity is divided by the protein concentration in solution (c). For the immobilized enzyme, the volumetric activity (U/mL) is multiplied by the immobilization yield (Y) and the dilution factor (D). Following this is divided by 100 for the yield and by the enzyme loading on the carrier.*

$$(a)\ \ sA(^{U}/_{mg}) = \frac{^{U}/_{mL}}{c(^{mg}/_{mL})}$$

$$(b)\ \ sAi\ (^{U}/_{mg}) = \frac{^{U}/_{mL} * D * Y(\%)}{100 * c(^{mg}/_{mL})}$$

- Final expressed activity

  The final expressed activity determines the activity of enzyme immobilized on the carrier per g of carrier ($U/g_{carrier}$).
- Relative recovered Activity

  It is the recovered activity in percent after immobilization. This is calculated by dividing the specific activity of immobilized enzyme by the specific activity in solution, multiplied by 100.
- Activity measured by oxygen sensing

  The slope of oxygen consumption within the reaction is used to calculate the volumetric activity (**Equation 5**)

Equation 5 Calculation of volumetric activity using the slope of oxygen consumption.

$$Volumetric\ Activity\ (^{U}/_{mL}) = \frac{(decrease\ of\ O_2\ (^{\mu mol}/_{L * min})) * (total\ reaction\ Volume\ (mL))}{(Volume\ of\ Suspension\ (mL)) * 1000\ mL/L}$$

Using the volumetric activity, the activity per g carrier can be evaluated using **Equation 6**.

Equation 6 Activity per g carrier using the oxygen consumption as an indicator of NOX activity.

$$Activity\ per\ g\ carrier\ (^{U}/_{g}) = Volumetric\ activity\ (^{U}/_{mL}) * Suspension\ factor\ (^{mL}/_{g})$$

Finally, the effectiveness factor (%) is calculated by dividing the activity of the immobilized NOX ($U/g_{carrier}$) by the offered activity (specific activity (U/mg) of

soluble NOX multiplied by the offered enzyme loading (mg/g)) and multiplied by 100.

- Normalization of NADH consumption observed under the microplate reader
  The absorbance of NADH is monitored over the reaction of NOX and the absorbance is subsequently normalized. Each measurement is divided by the starting point. In this case, the first measurement is 1 and every other point following is lower than 1 because NADH is consumed in the case of NOX.

2.2.6.5 PEI-coating

To coat the carrier with PEI, three PEI with different molecular weight (25 kDa, 60 kDa and 10^6 kDa) are tested. A solution of 10 mg/mL PEI in 100 mM sodium bicarbonate at pH 10 is prepared. After the enzyme is proven to be immobilized on the carrier, the supernatant is removed and the reaction solution with PEI is added as followed. Per 1 g of carrier, 10 mL of 10 mg/mL PEI solution is incubated for 1 hour. Afterwards, the supernatant is discarded and the carrier is reduced with freshly prepared 1 mg/mL sodium borohydride solution in the same ratio (1:10). Afterwards, the carrier is washed 3 times with 25 mM sodium phosphate buffer at pH 7 [44], [56].

2.2.6.6 Cofactor immobilization

For cofactor immobilization, the immobilized NOX coated with PEI is used. The carrier coated with PEI is pre-washed with 10 mM sodium phosphate buffer at pH 7. A solution of 1 mM NADH or FAD in 10 mM sodium phosphate buffer at pH 7 is prepared. This solution is incubated with the carrier in a suspension ratio of 1 to 10 for 1 hour. The carrier is washed 3 times with 10 mM sodium phosphate buffer at pH 7. To quantify the immobilized cofactor, the absorbance of cofactor solution before and after incubation is measured photometrically at 340 nm for NADH and at 450 nm for FAD [44].

2.2.6.7 Characterization of cofactor immobilization

The dissociation constant describes the ability to adsorb substances [57]. In our case, PEI is used to reversibly bind cofactors [56].

Therefore, agarose is coated with different PEI coatings of 3 different molecular weights, 25 kDa, 60 kDa and 10^6 kDa. The coating is done as described above. Next, each cofactor, FAD and NADH is immobilized in different concentrations starting with 0.1 mM up to a concentration of 30 mM as described above. Samples of the starting

solution and of the supernatant after immobilization are measured photometrically at 340 nm for NADH and at 450 nm for FAD. The cofactor concentrations are calibrated by plotting the unknown concentration against the absorbance of known cofactor concentrations. Using the initial and final absorbance, the adsorbed and non-adsorbed cofactor concentration are determined at the steady-state and plotted against each other. Afterwards, the K_d and Q(max) are calculated according to the Langmuir adsorption model (**Equation 7**) using the Origin software [57]:

Equation 7 Dissociation constant, K_d. *The adsorption of a substance (Q) is described by multiplying the maximal possible adsorption (Q(max)) and the concentration of the substrate. This is divided by the sum of substance concentration at half of the adsorption (K_d) and the substance concentration.*

$$Q = \frac{Q(\max) * S}{K_d + S}$$

2.2.6.8 Co-Immobilization of HRP-biotin via avidin

Avidin is used for binding of biotin related proteins. In our case, HRP is biotinylated. First of all, the immobilization of avidin is performed as for NOX. 1 mg/g avidin is immobilized on AG-Gx. To detect the best way of immobilization, different preparations of co-immobilized NOX and avidin are done:

- Avidin and NOX (1 mg/g each) immobilized simultaneously on AG-Gx
- NOX (1 mg/g) immobilized first and afterwards avidin (1 mg/g) on AG-Gx
- Avidin (1 mg/g) immobilized first and afterwards NOX (1 mg/g) on AG-Gx

In order to check the immobilization yield of each protein, samples are taken of immobilized avidin before NOX is immobilized and also immobilized NOX before avidin is immobilized.

For the immobilization of avidin, 0.1 mg/mL of avidin solution is prepared in 100 mM sodium bicarbonate buffer at pH 10. The carrier is incubated with the avidin solution for 1 hour under orbital shaking. After one hour, the immobilization yield is determined by using the Bradford assay. Finally, the carrier is reduced as described in the section “Immobilization of NOX”. For the HRP experiment, we prepared different carriers:

- NOX (1 mg/g) + PEI25 + Avidin (1 mg/g) + HRP-biot.
- NOX-Avidin (simultaneously, 1 mg/g each) + PEI25 + HRP-biot.
- NOX (1 mg/g)
- Avidin (1 mg/g) + HRP-biot.
- NOX-Avidin (simultaneously, 1 mg/g each) + HRP

The last three preparations are done as control. The sample with avidin and HRP is used as comparison of the immobilization process in absence of NOX. The last preparation should show that HRP does not bind to avidin if it does not contain biotin.

To bind HRP, the enzyme is related to biotin. The amount of biotinylated HRP for the co-immobilization can be calculated by the amount of immobilized avidin. The number of HRP-biotin molecules which can be bound onto the carrier is calculated using **Equation 8**:

Equation 8 Calculation of number of avidin molecules (N(protein)) immobilized on the carrier in total. *The immobilization yield (Y) is described elsewhere, the molecular weight of avidin is 26,000 g/mol and Avogadro constant determines the number 6.022*10^{23} mol^{-1}*

$$N(proteins) = \frac{offered\ Avidin(g) * Y(\%)}{MW_{Avidin}\ {}^{g}/_{mol}} * 6.022 * 10^{23}(mol^{-1})$$

The number of immobilized avidin can be multiplied by 4 because of the numbers of biotin binding sites. A similar equation can be used to calculate the number of molecules of HRP that can be immobilized (MW_{HRP}=80,000 g/mol).

2.2.7 Analysis of the protein distribution.

2.2.7.1 Fluorophore-Labelling (NOX and avidin)

NOX and avidin are labelled with two different fluorophores for fluorescence microscopy analysis as described elsewhere [44], [58]. NOX is labelled with rhodamine B isothiocyanate (rhodamine) as well as with FITC for two different experiments. Avidin is labelled with rhodamine.

For labelling, the molar ratio of the fluorophore and the protein is 1 to 1. Therefore, the molarity has to be calculated. Rhodamine has 536.08 g/mol, FITC has 389.38 g/mol, NOX has 27,000 g/mol per subunit and avidin has 68,000 g/mol per subunit. It has to be considered that NOX is a dimer and avidin is a tetramer. Because of that, the molar weight has to be multiplied by the number of subunits.

According to the calculated volumes and dilutions, the fluorophore and proteins are diluted in 100 mM sodium bicarbonate buffer at pH 8. The protein-fluorophore solution is incubated at room temperature under orbital shaking and in darkness for 1 hour. Afterwards, the solution is transferred into a column which contains a 10 kDa cut-off membrane. This is centrifuged 12,500 rpm for 10 minutes and the flow-through is discarded to separate the protein from the solution. For washing, 100 mM sodium bicarbonate buffer at pH 8 is added to the column and centrifuged until no color is in the supernatant. Afterwards, the proteins in the tube are resuspended in 200 µL of 100 mM bicarbonate buffer at pH 10 and transferred into a new tube. This buffer is used for immobilization as the enzymes are immobilized in the next step. Before that, the protein concentration is determined with the Bradford assay [44], [58].

2.2.7.2 Confocal microscopy

To visualize the distribution of NOX and avidin on AG-Gx and PU-Gx for several experiments, the confocal microscope ZEISS LSM 880 is used. NOX has intrinsically bound FAD which is autofluorescent and it can be used as an indicator of NOX. To monitor FAD and FITC, an argon laser with a filter MBS488/561 and a detector 499-570 nm is used as both are green emitting fluorophores (λ_{ex}: 488 nm). For Rhodamine, a DPSS 561/10 laser with a filter MBS488/561 and a detector 574-712 nm was used. For the samples immobilized on PU-Gx, 50% glycerine is added to the preparation to match the refraction index of the material with the medium.

The images are analysed and created with the program Fiji.

3 Results and Discussion

3.1 Preparation of immobilized NOX

The immobilization of NOX has been previously described by Rocha-Martín *et al.* [33]. In this work, we studied different parameters like the material of the support and the distribution of the immobilized enzyme and how that affects the catalytic properties of the immobilized NOX.

3.1.1 Expression and purification of NOX

To improve the expression of NOX in *E. coli* BL21, LB and TB media were compared. Expression, sonication and purification took place under the same conditions (Material and Methods). Aliquots of each purification step were applied on a SDS-PAGE which is depicted in **Figure 3**.

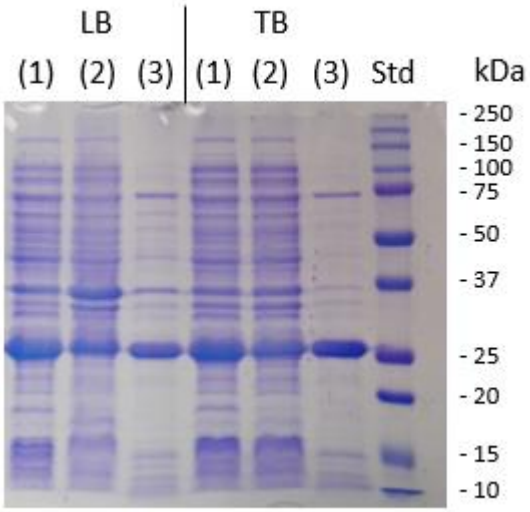

Figure 3 SDS-PAGE of the comparison of the different expression levels using LB and TB media. *Aliquots of each purification step were taken to compare the expression of NOX. As labeled above, samples are as follows for LB and TB media: (1) cell lysate, (2) soluble proteins, (3) proteins after thermal treatment. The most right shows a molecular weight marker (Std).*

As confirmed by SDS-PAGE (**Figure 3**), NOX was properly overexpressed in both media. Moreover, NOX remained in the soluble fraction after centrifugation and it was partially purified after thermal treatment. The major band shown in line 3 of TB and LB corresponds to the expected molecular weight of NOX (27 kDa) [33]. This indicates that the protein was properly overexpressed and purified. Comparing the heat-treated NOX expressed in LB and TB, the expression of the protein is very similar in both media. The protein concentration and the specific activity of NOX was then measured as described in Material and Methods (**Table 1**).

Table 1 Comparison of protein expression in E. coli in different media. *Protein concentration and activity expressed using LB are shown in Entry 1 and those expressed using TB are shown in Entry 2.*

Entry	Protein concentration (mg/mL)	Specific activity (U/mg)
1	0.711	29
2	0.597	37

After the heat treatment, higher a protein concentration could be found in samples from *E. coli* grown in LB media than in TB media. However, the specific activity of NOX expressed in TB media was higher than in LB media. As indicated by the SDS-PAGE and the specific activity, TB media is more advantageous than LB media for the expression. Thus, for all further experiments TB media was used.

3.1.2 Immobilization of NOX onto glyoxyl-activated materials

As discussed in the introduction, immobilization has several positive effects such as enhanced stability of enzymes and reusability. Rocha-Martín *et al*. described the immobilization of NOX employing different methods [33]. In this thesis, we are focusing on immobilization of NOX on glyoxyl activated carriers. Two different carrier materials are compared, agarose (AG-Gx) and methacrylate (PU-Gx). Our goal is to gain further knowledge about the catalytic properties of NOX immobilized on different carriers and how they influence the activity of the enzyme.

NOX was immobilized on AG-Gx and PU-Gx as described in Materials and Methods. The activity of the immobilized enzyme was measured by observing NADH consumption in a microplate reader. The results are summarized in **Table 2**.

Table 2 Immobilization parameters of immobilized NOX on different materials. *0.1 mg/g NOX were immobilized on AG-Gx (Entry 1) and PU-Gx (Entry 2), respectively. The suspension of the reaction mixture was 1:10. The specific activity of free NOX immobilized on AG-Gx was 19.81 U/mg and the specific activity of NOX immobilized on PU-Gx was 23.31 U/mg.*

Entry	Immobilization Yield (%)	Specific Activity (U/mg)	Expressed Activity ($U/g_{carrier}$)	Relative recovered Activity (%)
1	97.07 ± 0.05	**1.17 ± 0.11**	0.12 ± 0.01	6.27 ± 0.58
2	100	**2.23 ± 0.16**	0.22 ± 0.02	9.56 ± 0.67

Both enzyme preparations were immobilized following the same protocol. The relative recovered activity indicates that the immobilization process results in a high activity loss compared to the soluble enzyme. Interestingly, NOX immobilized on PU-Gx showed a higher catalytic performance than NOX immobilized on AG-Gx. Further experiments were conducted to gain insight in the difference of both materials under varying conditions.

3.1.3 Influence of cofactor presence during immobilization

In order to optimize the recovered activity of immobilized NOX, we tested the effect of the addition of cofactors (FAD and NADH) during the immobilization procedure. We hypothesize, the presence of these cofactors should protect the active site during the immobilization process, thus enhancing the relative recovered activity. Samples were prepared as described in Material and Methods: "Normal" (adding no cofactors), "FAD" and "FAD + NADH". After adding 1 mg/g of NOX to PU-Gx, the immobilization yield and the immobilized activity were determined (**Table 3**).

Table 3 Characterization of the heterogeneous biocatalysts after NOX immobilization on PU-Gx in different immobilization solutions. *Entry 1 was prepared following the original protocol (Normal) [33], [44]. Entry 2 (FAD) was prepared in the presence of additional FAD (0.15 mM. Entry 3 (FAD + NADH) was prepared in the presence of additional FAD (0.15 mM) and NADH (0.2 mM). The specific activity of free NOX was 9.26 U/mg for "Normal", 4.00 U/mg for "FAD" and 4.59 U/mg for "FAD + NADH".*

Entry	Additive	Immobilization Yield (%)	Specific Activity (U/mg)	Expressed Activity ($U/g_{carrier}$)	Relative Recovered Activity (%)
1	-	99.77	**0.38 ± 0.29**	9.34	4.03± 3.15
2	FAD	99.63	**0.15 ± 0.09**	8.18	4.64 ± 0.65
3	FAD + NADH	99.45	**0.07 ± 0.01**	6.21	2.27 ± 0.31

All the preparation methods showed a low specific immobilized activity. Moreover, no significant improvement was observed when adding either FAD or FAD + NADH. Because of that, all further immobilizations were done following the original protocol [33], [44]. Thus, other parameters must be responsible for the low recovered activities. The enzyme distribution onto the carrier has been described to have an impact on the catalytic performance of the biocatalyst [44]. To have a broader perspective on the immobilized enzyme, we further studied the different distributions of NOX onto the carriers.

3.2 Modulation of the protein distribution onto glyoxyl-activated materials

Varying the protein distribution on the carrier can affect the activity of the immobilized enzyme [22]. By slowing down the immobilization process, the enzyme might diffuse to the inside of the carrier. This allows for a more uniform distribution. In previous experiments, hydroxylamine was used to slow down immobilization on AG-Gx [44]. Hydroxylamine competes with NOX for the glyoxyl groups, thus slowing down the enzyme immobilization rate [44]. From this starting point, the immobilization of NOX on PU-Gx in the presence of various molecules was tested in hopes to achieve a uniform (homogeneous) distribution of NOX on the carrier.

3.2.1 Influence of Ethanolamine on the distribution of NOX on PU-Gx

Firstly, the effect of ethanolamine on the enzyme distribution on PU-Gx was tested. The immobilization course was followed by measuring the protein concentration in the bulk solution over time.

Three different immobilization protocols were followed as described in Material and Methods. For each sample, 1 mg of NOX was offered per g of PU-Gx carrier. In the protocol labeled “fast” no additives were employed. The other samples were immobilized with an additional 10 mM and 100 mM ethanolamine, respectively, following the immobilization protocol labeled “slow”. The results of the immobilization process are presented in **Figure 4**.

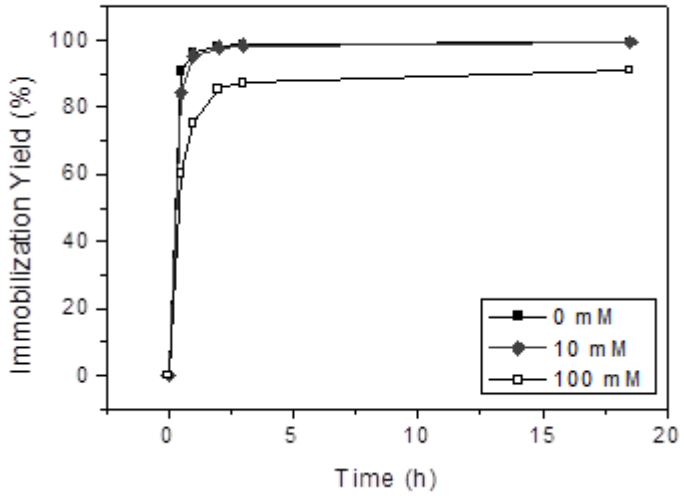

Figure 4 Immobilization kinetics of NOX on PU-Gx at varying ethanolamine concentrations. *Aliquots were taken periodically during the immobilization process to perform an activity assay. Remaining activity is plotted against time. The original immobilization did not contain any additives (0 mM). The other two samples contained additionally 10 mM ethanolamine and 100 mM ethanolamine.*

At lower concertation of ethanolamine (10 mM), the immobilization rate of NOX on PU-Gx is unaffected in comparison to the original immobilization protocol without additional ethanolamine. At higher ethanolamine concentration (100 mM), the immobilization rate of NOX was found to decrease. However, the effect of slowing down of ethanolamine on immobilization was to a lower extent than expected. A possible explanation for this may be the hydrophobic properties of PU-Gx. This can promote a rapid physical adsorption of the protein, hindering the effect of the ethanolamine. In contrast to the immobilization on agarose (e.g. AG-Gx), the immobilization on PU-Gx seems to be mainly driven by the hydrophobic interactions.

3.2.2 Influence of Hydroxylamine on the distribution of NOX on PU-Gx

As mention above, hydroxylamine is known to slow down the immobilization process of NOX on AG-Gx [44]. Thus, the effect of hydroxylamine for the immobilization of NOX on PU-Gx was tested.

In this experiment, two different enzyme loadings were compared (0.1 mg/g carrier and 3 mg/g carrier). This was done to investigate the impact of enzyme loading on the immobilization to obtain a homogeneous distribution on the carrier. To slow down the immobilization, hydroxylamine was added to the immobilization reaction solution so to obtain a final concentration of 10 mM of hydroxylamine. The immobilization was observed for 21 hours (**Figure 5**).

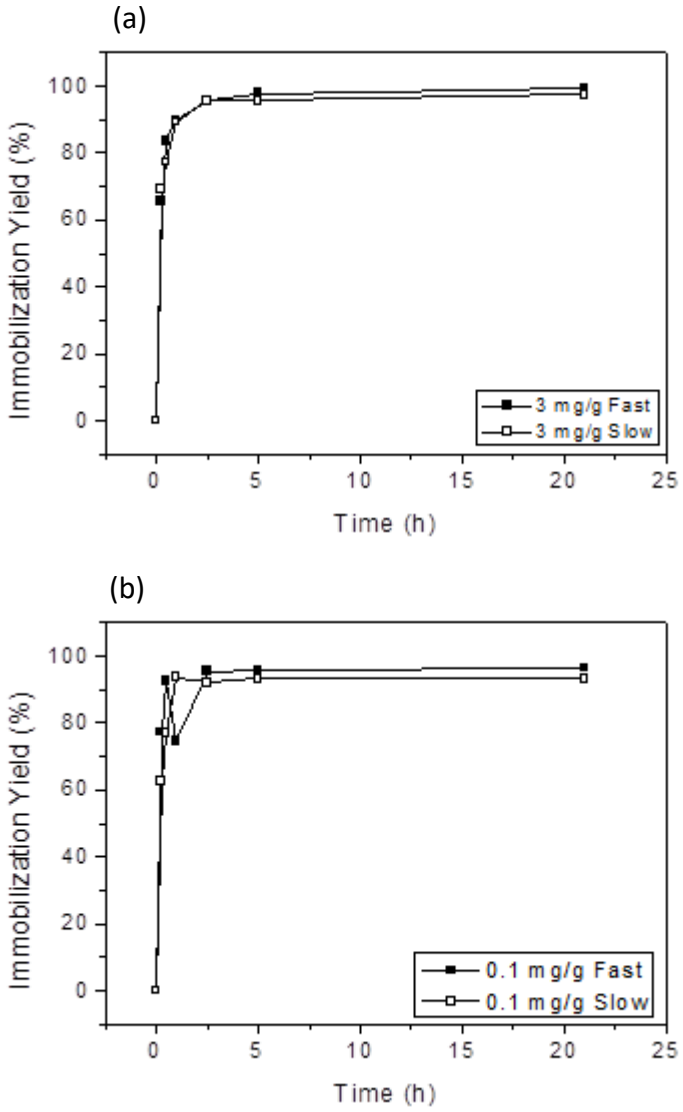

Figure 5 Influence of hydroxylamine on the immobilization kinetics of NOX on PU-Gx. *The "fast" immobilized NOX (dark squares) followed original immobilization protocol. The "slow" one (white squares) contained 10 mM hydroxylamine to slow down the immobilization process.*

At both high and low protein loading conditions, hydroxylamine had a negligible effect on the immobilization rate. This is indicated by the similar immobilization yields obtained for both preparation protocols, with and without addition of hydroxylamine. Moreover, the first sample was taken after 1 h of incubation, at which time the enzyme might already be immobilized. The samples should have been taken in shorter intervals at the beginning of the immobilization process to make out a noticeable difference. In comparison to ethanolamine, hydroxylamine interferes less with the immobilization of NOX on PU-Gx. Contrary to our expectations, hydroxylamine does not seem to be a suitable reagent to slow down the immobilization of NOX. As mentioned above, the hydrophobic nature of PU-Gx may influence the immobilization of NOX by adsorption.

Furthermore, hydroxylamine is more hydrophilic than ethanolamine which could explain why ethanolamine slows down the immobilization of NOX, while hydroxylamine does not.

3.2.3 Ethanol as a tool to slow down the immobilization

The hydrophobic characteristics of PU-Gx complicate homogenous distributions following same methodologies as for AG-Gx. Previously, ethanol has been used to slow down the immobilization process under hydrophobic conditions [55]. To improve homogenous distribution of NOX on the carrier, we tried to adapt to these principles.

To do so, the slow immobilization of NOX was tested in the presence of 10 mM hydroxylamine and additional 30% (v/v) of ethanol to prevent hydrophobic interactions. **Figure 6** shows the immobilization yield course of NOX on PU-Gx.

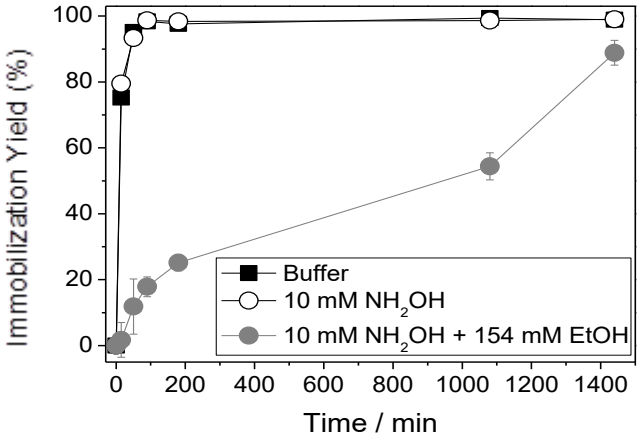

Figure 6 Comparison of different immobilization protocols of NOX on PU-Gx. *NOX was immobilized without additives (buffer), with additional 10 mM hydroxylamine (10 mM NH2OH) and with additional 10 mM hydroxylamine and 30% (v/v) ethanol (10 mM NH2OH + 154 mM EtOH). This experiment was carried out by Dr. Benítez-Mateos.*

The addition of ethanol and hydroxylamine slows down the immobilization process. The immobilization process was incubated for more than 23 hours after which the immobilization yield reached approximately 90 %. In comparison, when only hydroxylamine was added, it did not have an impact on the immobilization.

Next, we could demonstrate that 30 % ethanol (v/v) does not denature the enzyme. Therefore, the consumption of NADH of each catalyst preparation variation was assayed. The normalized absorbance of the cofactor over time is shown in **Figure 7**.

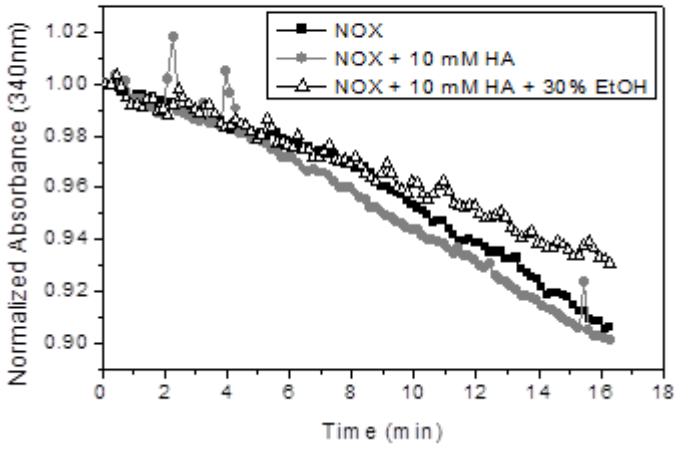

Figure 7 Impact of ethanol on the distribution of NOX on PU-Gx as observed by NADH consumption of NOX over time. *The dark grey spares correspond to the sample without additives (fast). The light grey circles correspond the samples containing 10 mM hydroxylamine. The white triangles correspond to the slow sample with 10 mM hydroxylamine and 30% (v/v) ethanol.*

The rate of consumption of NADH correlates to the activity of the biocatalyst after immobilization. The addition of ethanol only marginally decreased catalyst activity compared to either samples prepared without additives, or 10 mM hydroxylamine, respectively. Therefore, NOX did not seem to be inactivated by treatment with ethanol. To demonstrate that the different immobilization methods have an effect on the distribution of the enzyme, the different samples of immobilized NOX on PU-Gx were visualized using confocal fluorescence microscopy. As FAD is auto-fluorescent, this cofactor intrinsically bound to the enzyme can be used as an indicator in fluorescence microscopy. This allows for the visualization of the enzyme on the carrier without the need for any further labeling. **Figure 8** shows the spatial distribution of NOX on PU-Gx following the different immobilization protocols.

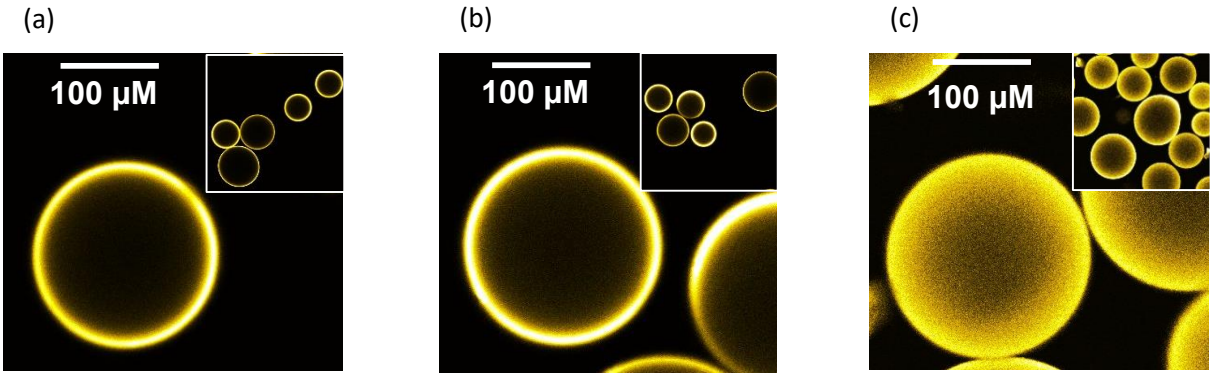

Figure 8 Spatial distribution of NOX immobilized on PU-Gx. *The samples were immobilized following different immobilization protocols: (a) NOX on PU-Gx without additives, (b) NOX on PU-Gx with 10 mM hydroxylamine and (c) NOX on PU-Gx with 10 mM hydroxylamine and 30% (v/v) ethanol. Images were edited by Dr. Benítez-Mateos.*

The microscopy images indicate that the distribution of NOX on PU-Gx with additional hydroxylamine is similar to the preparation without additives. This correlates with the immobilization yield observed before. The sample prepared in the presence of hydroxylamine and ethanol shows the distribution of NOX onto the carrier is uniform as can be inferred from the immobilization yield.

Overall, the combination of hydroxylamine and ethanol slows down the immobilization of NOX on PU-Gx by overcoming the hydrophobic interactions of the carrier with the enzyme. The microscopy images demonstrate that NOX is distributed homogenously within the carrier. Even though a small activity loss was observed in the presence of ethanol, the slow immobilization method seems to be the ideal option to obtain homogeneous distribution on the purolite carrier.

3.3 Effect of spatial distribution, enzyme density and mixing on the recovered activity of the immobilized enzyme

So far, we established the effect of ethanol and hydroxylamine on a homogenous distribution on PU-Gx. In this section, we present the impact of varying enzyme loadings and distributions of the enzyme on PU-Gx on the activity. Additionally, we discuss the impact of different mixing methods using orbital shaking and magnetic stirring. We also compare both materials, AG-Gx and PU-Gx, and their properties according to the specific activity of NOX under the different mixing methods. By doing so, we hope to gain a better understanding of the limiting factors under different conditions.

3.3.1 The impact of different mixing methods on the catalytic performance of NOX immobilized on PU-Gx

In a suspension of immobilized enzyme, the proper mixing of the reaction mixture may have a great impact on the activity of the enzyme. Sufficient mixing provides good dispersion of the carrier in the fluid and thus external transport of the reactants to the immobilized enzyme is facilitated [18, p. 255]. Thus, we aimed to understand the impact of different mixing methods on the biocatalytic performance of the enzyme. Moreover, different enzyme loadings on PU-Gx were tested.

To do so, NOX was immobilized in two different concentrations on PU-Gx and the reaction mixtures were subjected to one of two mixing method: orbital shaking, or magnetic stirring. Enzyme activity was determined by measuring NADH consumption. Orbital shaking is induced by the microplate reader. In the case of magnetic stirring, samples were measured in the photometer in which an external magnetic stirrer system was incorporated. This allows a continuous, vigorous mixing during the measurements. The measurements are summarized in **Table 4**.

Table 4 Comparison of different mixing methods and their impact on the activity of immobilized NOX on PU-Gx. *The suspension of the reaction mixture was 1:10. The soluble enzyme had a specific activity of 23.31 U/mg in case of orbital shaking, and 15.52 U/mg in the case of magnetic stirring, respectively. Entry 1 and 2 show the activities from 0.1 mg/g NOX and Entry 3 and 4 show the activities from 3 mg/g NOX.*

Entry	Mixing Mode	Immo-bilization Yield (%)	Specific Activity (U/mg)	Expressed Activity ($U/g_{carrier}$)	Relative Recovered Activity (%)
1	Orbital Shaking	100.00	**2.23 ± 0.16**	0.22 ± 0.02	9.56 ± 0.67
2	Magnetic Stirring		**3.34 ± 0.32**	0.38 ± 0.08	21.50 ± 2.03
3	Orbital Shaking	90.57	**0.15 ± 0.07**	0.48 ± 0.24	0.63 ± 0.31
4	Magnetic Stirring		**0.54 ± 0.08**	1.78 ± 0.26	3.46 ± 0.51

All mentioned data and activities were calculated as described in Material and Methods. It has to be mentioned that the activity of NOX (free and immobilized) measured under magnetic stirring were observed a few days later than the samples under orbital shaking. This resulted in a lower specific activity of the soluble enzyme under magnetic stirring compared to the samples measured under orbital shaking as the activity of soluble NOX decreases over time. As immobilization generally has a

stabilizing effect on enzymes, it can be expected that storage of the immobilized NOX for several days did not affect its specific activity to such an extend as soluble NOX.

In all cases, higher activities were found in the samples mixed by magnetic stirring rather than orbital shaking. This seems to be due to improved mixing in the system. At low enzyme loading (0.1 mg/g) a higher specific activity and a higher relative recovered activity were found compared to high enzyme loading (3 mg/g). The mass transfer of the cofactors and substrate appears to be much better for the low enzyme loading than for high enzyme loading. A reason for this might be the wider distribution of NOX on the carrier which results in a better activity because of the mitigated mass transfer limitations of both, cofactor and oxygen. In comparison, at high enzyme loadings NOX, the mitigation of the external mass transfer resistance is not enough. This leads to the enzyme not being fully utilized. Thus, the low loading is expected to achieve a higher catalytic performance.

Overall, the data (**Table 4**) shows that improved mixing enhances the external mass transfer and thus the activity of NOX. Nevertheless, the improvement of mixing does not seem to affect high loadings as efficient as low loadings. For this reason, we are going to investigate the intrinsic properties of the different supports. These properties might be another parameter affecting the mass transfer of substrates and cofactors.

3.3.2 Effects of the material properties on the performance of immobilized NOX

Due to the different physico-chemical properties of both supports (AG-Gx and Pu-Gx), we studied the impact of mixing on the specific activity of immobilized NOX onto each support. As shown in section 3.1, low protein loading showed higher overall activity. To study the effect of carrier properties and mixing modes, 0.1 mg/g NOX was immobilized onto AG-Gx as well as PU-Gx in a “fast” manner. Enzyme activity was again measured as described in the section above. The immobilization and the observed activities on NOX on AG-Gx are summarized in **Table 5**.

Table 5 Comparison of different mixing methods for NOX immobilized on AG-Gx at 0.1 mg/g. *The suspension mixture of reaction mixture and carrier was 1:10. The soluble enzyme had a specific activity of 19.81 U/mg in the case of orbital shaking and 29.95 U/mg in the case of magnetic stirring.*

Entry	Mixing Mode	Immo-bilization Yield (%)	Specific Activity (U/mg)	Expressed Activity ($U/g_{carrier}$)	Relative recovered Activity (%)
1	Orbital Shaking	97.07 ± 0.05	**1.17 ± 0.11**	0.12 ± 0.01	5.91 ± 0.54
2	Magnetic Stirring	97.07 ± 0.05	**9.29 ± 1.81**	0.96 ± 0.19	31.00 ± 6.03

Similar to previous experiments employing Pu-Gx, the difference between specific activity with orbital shaking and magnetic stirring is also substantial when using AG-Gx as a support. Magnetic stirring promoted higher specific activity and relative recovered activity. The samples measured with magnetic stirring showed an 8-fold higher specific activity than the ones measured with orbital shaking. Moreover, the relative recovered activity differed at a factor of 4.2. To visualize the difference as well as the effect of the different carrier, the specific activity of NOX on PU-Gx (**Table 4**) and AG-Gx (**Table 5**) is plotted (**Figure 9**).

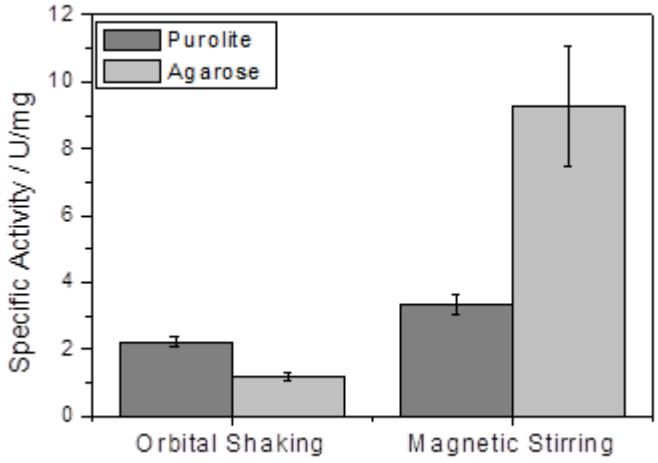

Figure 9 Comparison of specific activity of NOX on different carriers under different mixing conditions. *0.1 mg/g NOX on PU-Gx (dark grey) and on AG-Gx (light grey) are plotted.*

In **Figure 9**, the specific activities of immobilized NOX on the two carriers using different mixing methods can be seen. Both enzyme preparations obtained higher activity by magnetic stirring.

As discussed in section 3.1, major mass transfer limitations of substrate and cofactors are mitigated by magnetic stirring. This results in an observable increase of NOX activity. Especially, NOX on AG-Gx showed an 8-fold increase when applying more vigorous mixing. In comparison, the activity obtained by NOX on PU-Gx increases only marginally. This hints towards the carrier material also having an influence on the mass transfer. AG-Gx is more hydrophilic than PU-Gx. This might influence the mass transfer of substrate and cofactor as well.

The unpolar oxygen molecules have a higher affinity towards hydrophobic environments. This might be a reason why the specific activity of NOX on PU-Gx is higher than on AG-Gx when applying orbital shaking. Contrastingly, the specific activity of NOX on AG-Gx increases by magnetic stirring. This leads to the hypothesis that over all mass transfer might be facilitated in hydrophilic agarose (AG-Gx) rather than PU-Gx. This results in the substantial increase of specific activity of NOX on AG-Gx. To gain a further knowledge about the limiting factors in the reaction, further experiments were conducted.

3.3.3 Effects of spatial distribution on the enzyme performance

As discussed in section 2.3, we could show that the presence of hydroxylamine and ethanol could slow the immobilization process down. This resulted in a homogenous distribution of the immobilized enzyme on Pu-Gx. Having this on hand, we proceeded to test the activities under different mixing conditions, orbital shaking and magnetic stirring. We set out to observe the effect of the two mixing methods on the biocatalytic activity of the immobilized enzyme in different spatial organizations.

The catalytic performances of the enzyme preparations with different distributions, heterogeneous (“F” for fast) and homogenous (“S” for slow), were tested under the two mixing conditions (**Table 6**).

Table 6 Impact of spatial distribution on the catalytic performance of 0.1 mg/g NOX immobilized on PU-Gx comparing different mixing methods. *The homogeneous (Entry 3 and 4) samples were prepared in the presence of 10 mM hydroxylamine and 30% (v/v) ethanol during the immobilization process. The heterogeneous catalyst (Entry 1 and 2) was prepared in the absences of any additives during the immobilization process. The reaction suspension was 1:5 for the orbital shaking and 1:10 for magnetic stirring. The soluble enzyme had a specific activity of 14.11 U/mg under orbital shaking and 12.31 U/mg under magnetic stirring.*

Entry	Mixing Mode	Immo-bilization Yield (%)	Specific Activity (U/mg)	Expressed Activity ($U/g_{carrier}$)	Relative Recovered Activity (%)
1	Orbital Shaking	99.75 ± 0.00	**0.75 ± 0.19**	0.08 ± 0.02	5.30 ± 1.40
2	Magnetic Stirring		**4.11 ± 0.55**	0.41 ± 0.05	33.38 ± 4.43
3	Orbital Shaking	97.49 ± 0.10	**1.08 ± 0.25**	0.11 ± 0.03	7.65 ± 1.73
4	Magnetic Stirring		**0.87 ± 0.27**	0.09 ± 0.03	7.09 ± 2.17

As expected, magnetic stirring increased the specific activity of heterogeneously immobilized NOX by a factor of 5.5 over orbital shaking. The comparison of the specific activities is depicted in **Figure 10**.

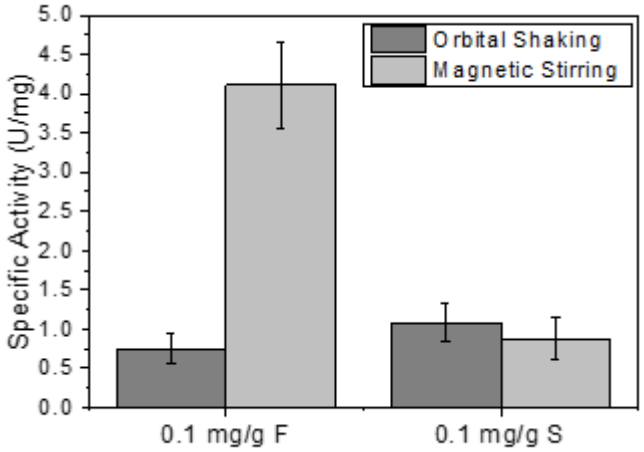

Figure 10 Effect of mixing mode on the specific activity of immobilized NOX with different spatial distribution. *The different distributions are marked with "F" for fast, heterogeneous which demonstrates a heterogeneous distribution and "S" for slow immobilization, which demonstrates a homogeneous distribution.*

The localization of the enzyme on the outer surface provides a better accessibility of cofactors and oxygen which are made even more accessible by vigorous mixing. In the case of homogeneous distribution, no significant difference in specific activity can be made out as the error bars overlap. Even though mixing is increased, mass transfer into the pores might not be sufficient enough. Therefore, the mass transfer of the substrates must be analyzed to understand the differences on the catalytic

performance. As the heterogeneous distributed NOX on PU-Gx achieved a higher activity, this preparation is studied further by increasing enzyme loading.

3.3.4 Observation of oxygen consumption in the reaction of NOX immobilized on PU-Gx

Oxygen consumption was observed by O_2 sensing in the bulk [43]. This was done to observe the substrate consumption and to analyze further limiting factors within the reaction. To do so, NOX was heterogeneously immobilized in two different concentrations onto PU-Gx. The catalytic activity of 0.1 mg/g NOX and 3 mg/g NOX immobilized on PU-Gx was monitored at two different concentrations of NADH (**Table 7**). All samples were mixed by magnetic stirring as it facilitates mass transfer more effectively than orbital shaking.

Table 7 Catalytic performance of NOX immobilized on PU-Gx by monitoring the oxygen consumption. *The oxygen consumption was measured in solution via oxygen sensing. The soluble NOX had a specific activity of 0.5 U/mg. The suspension was 1:10.*

Entry	Enzyme Loading	Offered Activity U/g	NADH (mM)	Activity in Solution ($U/g_{carrier}$)	Effectiveness Factor (%)
1	0.1 mg/g	0.05	0.2	0.13	250.17
2			3	0.28	567.44
3	3 mg/g	1.5	0.2	0.28	18.82
4			3	0.50	33.17

At high enzyme loading conditions (3 mg/g) expressed activity was higher than at the low enzyme loading conditions (0.1 mg/g). In addition, the activity increased by elevating NADH concentration in solution. Nevertheless, the effectiveness factor is lower for the high enzyme loading (Entry 3 and 4) rather than the low enzyme loading (Entry 1 and 2). This indicates that substrates might be limiting at high enzyme loading.

At low enzyme loadings, the substrates limitations seem to be negligible under magnetic stirring conditions. Whereas, at high enzyme loadings, the reaction is probably limited by both oxygen and NADH. A noticeable effect can be attributed to NADH, as an increase in NADH concentration in the reaction solution resulted in a

higher enzymatic activity in all cases. The limitation of activity by cofactors can be overcome by increasing the concentration of cofactor, however the cofactors are quite expensive and the cost-efficiency of the system would be pretty compromised.

3.4 Improvement of the activity of immobilized NOX

Enzyme activity is highly dependent on the cofactor concentration. To solve the problem of that dependency and to avoid the need of adding high concentration of cofactors, a co-immobilization approach is used. Velasco-Lozano *et al.* have reported that the cofactors can be reversibly attached to PEI (polyethyleneimine)-coated heterogeneous biocatalysts via ionic interactions [44], [56]. PEI facilitates the co-immobilization of enzymes and phosphorylated cofactors such as NADH and FAD, confining those ones within the porous surface and increasing their local concentration around the immobilized enzyme (**Figure 11**). This may enhance the reaction rate and mitigate the mass transport at both internal and external level [18], [56], [59].

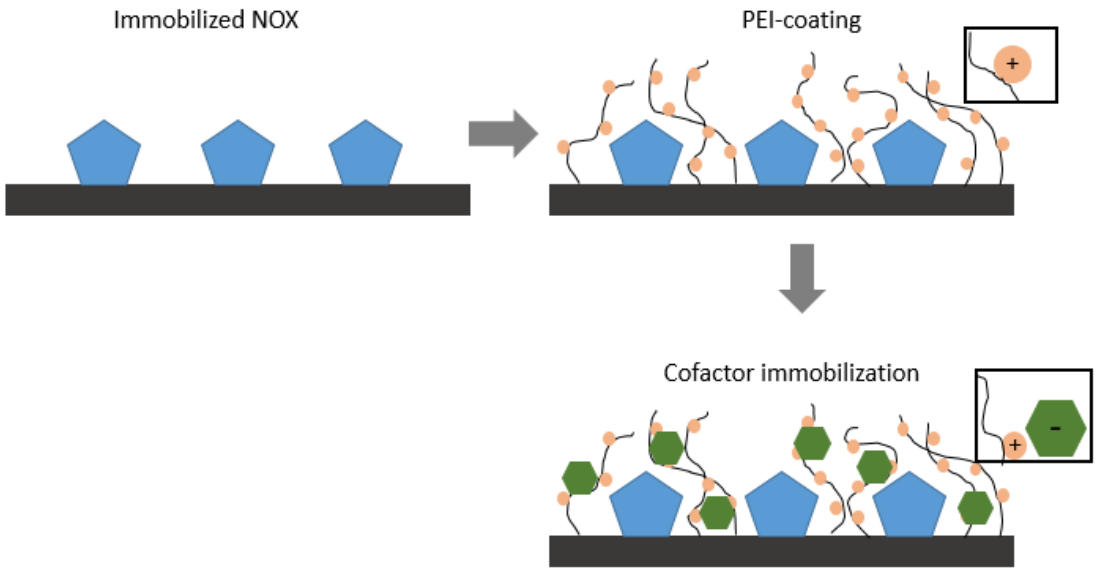

Figure 11 Scheme of cofactor co-immobilization. *The enzyme (blue) is immobilized onto a porous surface. The immobilized enzyme is coated with PEI (orange). Due to reversible ionic interactions, the cofactor (green) binds to the positively charged PEI.*

In this section, we describe the cofactor immobilization on different materials using different types of PEI and characterize the influence of PEI on the activity of immobilized NOX. We aimed to improve the catalytic performance by overcoming the mass transfer limitations of cofactors.

3.4.1 K_d of the cofactors on different PEI

First of all, we tested this hypothesis by characterization of the cofactor binding capacity of different PEIs through Langmuir adsorption experiments. The cofactors establish an association/dissociation equilibrium with the PEI. To obtain an enhanced knowledge about this interactions, we tested PEI of different sizes (25 kDa and 10^6 kDa) and determined the dissociation constant (K_d) which can be used to describe said equilibrium. In **Figure 12**, the bound NADH is plotted against the unbound NADH (in the supernatant).

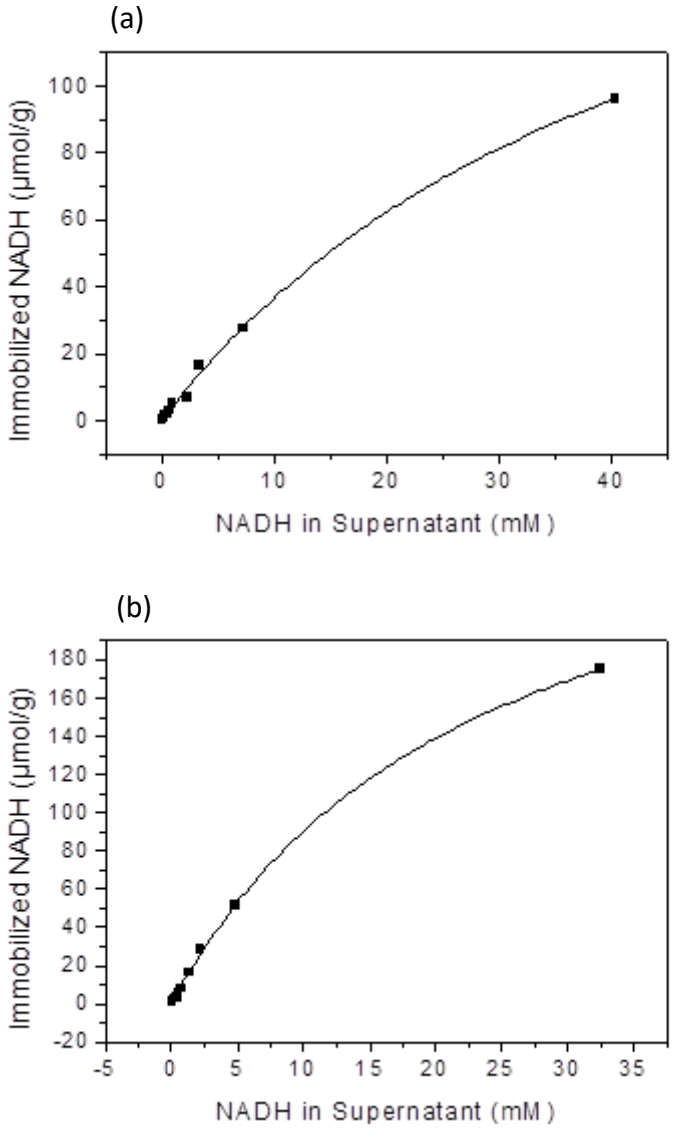

Figure 12 Langmuir curves of NADH immobilized on AG-Gx-PEI. *PEI of different molecular weight were tested: (a) 25 kDa and (b) 106 kDa. Kd and Q(max) are shown in* ***Table 8****. The NADH bound on AG-Gx-PEI is plotted against the remaining NADH concentration in the supernatant.*

The carrier was coated with PEI as described in Material and Methods. Different concentrations of NADH or FAD were subsequently incubated with AG-Gx-PEI. The absorbance of the initial NADH/FAD solution and the supernatant after cofactor immobilization were measured. This allows for the calculation of the concentration of cofactor bound and unbound at the absorption equilibrium. K_d and Q(max) are listed in **Table 8**.

Table 8 Q(max) and K_d of immobilized NADH on different PEI-coatings on AG-Gx. *The carrier was coated with 2 different PEI: PEI25 (Entry 1) and PEI106 (Entry 2). The values were calculated from the graphs (Figure 12) and the dissociation equation (**Equation 7**). The R2 in both cases was 0.99.*

Entry	Coating	Q(max) (µmol/g)	K_d (µmol/g)
1	PEI25	206.91 ± 16.57	46.39 ± 6.37
2	PEI10^6	299.49 ± 7.25	23.10 ± 1.15

As shown in **Figure 12** and **Table 8**, Q(max) increases with an increase of the molecular weight of PEI. The K_d decreases with higher molecular weight. The high Q(max) and the low K_d of PEI10^6 suggest that the polymer with the higher molecular weight binds the cofactor more strongly than the one with lower molecular weight. This means the cofactor is less likely to lixiviate from the beads. Simultaneously, the amount of cofactor available for the enzyme might be limited.

Next, the K_d of FAD was determined using 3 different PEIs (25 kDa, 60 kDa and 10^6 kDa). The Lagmuir curves to determine K_d and Q(max) are depicted in **Figure 13**. The same immobilization and evaluation protocol were followed as previously for NADH.

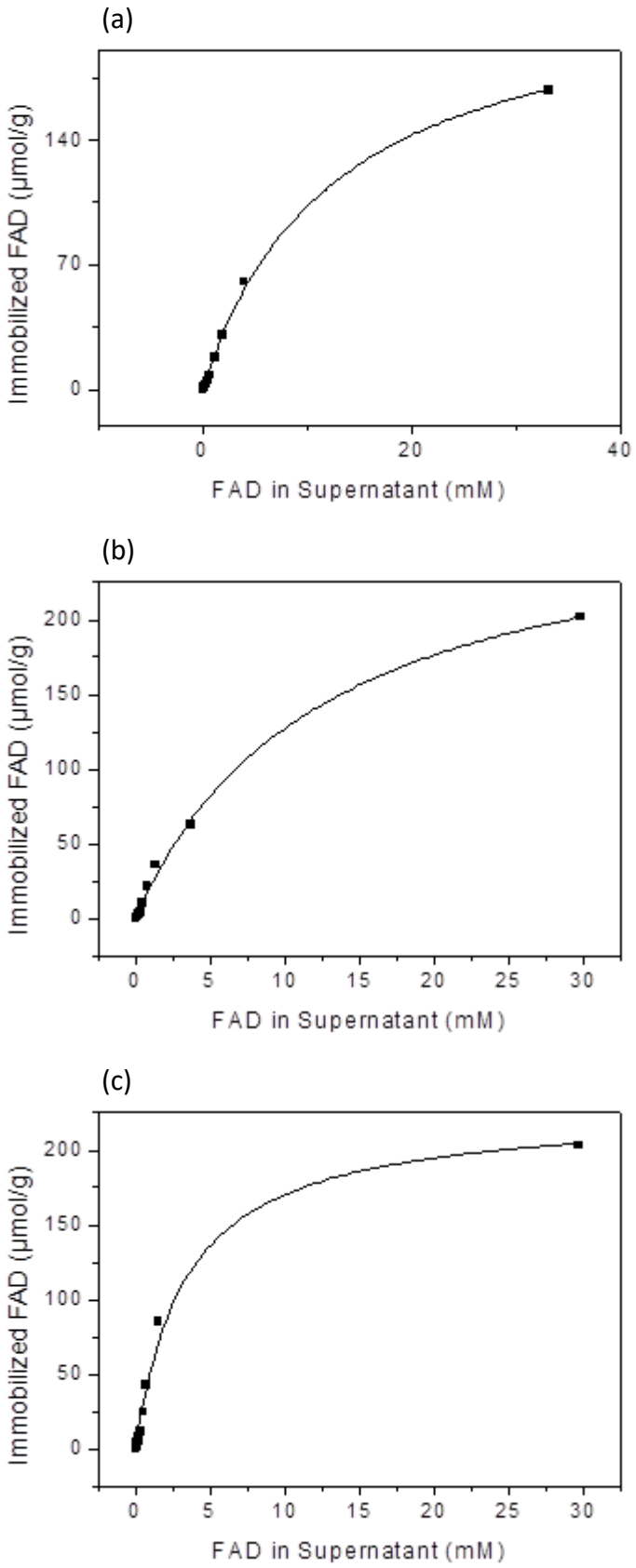

Figure 13 Lagmuir curves of FAD on different AG-Gx-PEI. *Different concentrations of FAD were immobilized on the carrier with (a) 25 kDa, (b) 60 kDa and (c) 106 kDa. Kd and Q(max) correlating to the plots are listed in* ***Table 9.***

The plateau of PEI25 and PEI10^6 are similar to each other. Q(max) as well as K_d are summarized in **Table 9**. As in the case of NADH, the K_d of FAD also decreased as the molecular weight of the PEI increased. The higher the molecular weight of the PEI coating, the stronger the cofactors bind. The K_d of PEI25 and PEI60 do not show a significant difference. However, both K_d are higher than the K_d of PEI10^6.

Table 9 Q(max) and K_d of FAD-immobilization onto different PEI coatings. *The carrier is coated with 3 different PEI: PEI25 (Entry 1), PEI60 (Entry 2) and PEI106 (Entry 3). The values were calculated by the slopes (**Figure 13**) using the dissociation equation (**Equation 7**). In all cases R2 > 0.9.*

Entry	Coating	Q(max) (µmol/g)	K_d (µmol/g)
1	PEI25	232.55 ± 8.90	12.63 ± 1.21
2	PEI60	286.56 ± 12.29	12.53 ± 1.35
3	PEI10^6	227.70 ± 11.09	3.39 ± 0.50

Comparing the dissociation constants within the different cofactors, the K_d of FAD (**Table 9**) is substantially lower than the K_d of NADH (**Table 8**) as it was previously reported elsewhere [56]. This could be a result of structural differences between the cofactors. Despite NADH as well as FAD possessing the same number of phosphate groups, which are similarly positioned in the molecule, the aromaticity is different. FAD has a more aromatic structure than NADH. This difference in aromaticity may explain additional hydrophobic interactions with PEI. In both cases, NADH and FAD, the K_d decreased as the PEI-weight increased with PEI10^6 exhibiting the highest binding affinity. This effect may be explained by the higher number of positively charged groups in the larger PEI. Consequently, the higher the molecular weight of the PEI, the higher the retention capacity of the cofactors. Additionally, the Q(max) did not vary too much between the PEIs. A reason for this is that theoretically the net charge of the polymer should be the same in all cases. Whereas, the density of the polymer varies and this might affect the dissociation constant. Because of that there is no clear trend noticeable.

The strategy of cofactor co-immobilization may be a tool to overcome the mass transfer limitations of cofactors. In the herein described experiments we additionally coated the carrier with PEI. As previously reported, the cofactor can interact with the PEI without a previous step of incubation with the cofactor for co-immobilization [44]. This should enhance the catalytic performance of immobilized NOX.

3.4.2 Impact of different mixing methods on the activity of high and low protein loading immobilized on PU-Gx and coated with PEI60

As discussed in section 4.1, PEI60 showed a higher cofactor loading capacity (**Table 9**). According to this, the immobilized enzyme was additionally coated with PEI60. Even though the cofactors were not co-immobilized on the carrier in this case, the PEI coating should enhance the binding affinity of cofactors and mitigate mass transfer limitations. The activity of NOX immobilized on PU-Gx-PEI is summarized in **Table 10**.

Table 10 Impact of different mixing methods (orbital shaking and magnetic stirring) on the activity of NOX immobilized on PU-Gx coated with PEI60*. 2 different enzyme loadings were immobilized: 0.1 mg/g NOX (Entry 1 and 2) and 3 mg/g NOX (Entry 3 and 4). The suspension of the reaction mixture was 1:10. The soluble enzyme had a specific activity of 23.31 U/mg under orbital shaking and under magnetic stirring 15.52 U/mg.*

Entry	Mixing Mode	Immo-bilization Yield (%)	Specific Activity (U/mg)	Expressed Activity ($U/g_{carrier}$)	Relative Recovered Activity (%)
1	Orbital Shaking	99.9	**4.70 ± 1.74**	0.47 ± 0.17	20.15 ± 7.46
2	Magnetic Stirring		**8.21 ± 0.85**	0.82 ± 0.09	52.87 ± 5.47
3	Orbital Shaking	99.8	**0.27 ± 0.05**	0.82 ± 0.16	1.17 ± 0.23
4	Magnetic Stirring		**1.13 ± 0.02**	3.40 ± 0.05	7.30 ± 0.10

Alike for the immobilized enzymes without PEI-coating (**Table 4**), 0.1 mg/g preparations exhibited a higher specific activity as well as a higher relative recovered activity compared to the high enzyme loading of 3 mg/g (**Table 10**). This indicates that a PEI-coating has an impact on the catalytic performance even without a previous co-immobilization step. The coating attracts the cofactors, thus facilitating mass transfer of NADH and FAD and overcoming those limitations. The biocatalyst with high enzyme loading has a significantly lower catalytic performance likely due to a drastic oxygen limitation within the reaction. The oxygen mass transfer into the carrier is slower than the enzyme consumes the oxygen resulting in a lower specific activity. The low enzyme loading is not as affected by these limitations as the high enzyme loading. Consequently, the low enzyme loading shows a higher catalytic performance which is even enhanced by the vigorous mixing under magnetic stirring conditions. Since PEI decreases cofactor limitations, we then compared different carrier materials, agarose and purolite, under the influence of the PEI coating.

3.4.3 Comparison of the catalytic performances of NOX immobilized on PU-Gx and AG-Gx with PEI-coating

To understand different behavior of the PEI-coating of agarose and purolite, NOX was immobilized on both carriers, AG-Gx and PU-Gx, and coated with PEI. This section aims to summarize our findings on the effect of PEI-coating on different materials under different mixing methods, as those materials exhibited slightly different properties described in section 3.2.

The catalytic performances of NOX immobilized on AG-Gx coated with PEI60 are summarized in **Table 11**.

Table 11 NOX immobilized on AG-Gx-PEI. *The suspension mixture of the reaction mixture and carrier was 1:10. The soluble NOX had a specific activity of 19.81 U/mg in the case of orbital shaking and 29.95 U/mg in the case of magnetic stirring.*

Entry	Mixing Mode	Immo-bilization Yield (%)	Specific Activity (U/mg)	Expressed Activity ($U/g_{carrier}$)	Relative recovered Activity (%)
1	Orbital Shaking	100.00	**1.67 ± 0.28**	0.17 ± 0.03	8.45 ± 1.43
2	Magnetic Stirring	100.00	**11.25 ± 2.04**	1.13 ± 0.20	37.58 ± 6.80

Both, the specific activity and the relative recovered activity, are higher under magnetic stirring conditions. As discussed in section 3, vigorous mixing overall enhances the catalytic performance of NOX and especially oxygen limitations are overcome. Moreover, PEI enhances mass transfer of cofactors which further improves NOX activity. Subsequently, we tested the effect of PEI-coating for the immobilized NOX on different materials. The comparison of the specific activity on NOX on AG-Gx-PEI and PU-Gx-PEI is depicted in **Figure 14**.

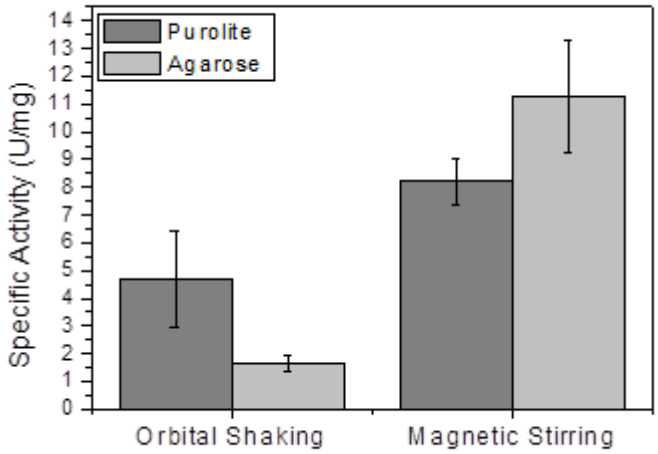

Figure 14 Comparison of specific activity of NOX immobilized on PU-Gx-PEI (dark grey) and AG-Gx-PEI (light grey). *The specific activities of NOX immobilized on PU-Gx are listed in Table 10 and the specific activity of NOX immobilized on AG-Gx are listed in* ***Table 11.***

Noteworthy, the ratios of the specific activities of NOX on purolite or agarose measured under orbital shaking and magnetic stirring are different (**Figure 14**). As discussed above in section 3.2, agarose is more hydrophilic and oxygen does not dissolve in this environment as well as in the hydrophobic environment of purolite. This limitation for agarose can be overcome by the increase of mixing (i.e. magnetic stirring over orbital shaking). Moreover, the PEI coating overall improved the availability of cofactors and the activity especially for agarose (**Figure 14**). Compared to section 3.2, the difference in specific activity for both carrier materials coated with PEI and under magnetic stirring was not as pronounced as without PEI. As purolite is more hydrophobic, oxygen may more easily diffuse into the carrier. Presence of PEI enhanced the mass transfer of cofactors which resulted in higher catalytic performances even under weak mixing conditions. Overall, the integration of PEI enhanced the accessibility of NADH and FAD in the microenvironment of the enzyme resulting in decreased limitation of cofactor accessibility. This improvement is substantial when using a hydrophilic material, like agarose, coated with PEI and operated with a good aeration system.

In addition, the impact of PEI-coating on the catalytic performance of NOX with varying spatial distributions would be of interest for a better understanding of the microenvironment of the enzyme.

3.4.4 Impact of the spatial distribution on the activity of NOX immobilized on PU-Gx-PEI

To observe the effect of PEI on the homogenous (slow immobilization) and heterogeneous (fast immobilization) distribution of NOX on PU-Gx, the activity was monitored. A PEI of lower molecular weight was chosen (25 kDa) because of the higher dissociation constant. The coating confines the cofactor in the surroundings of the enzyme, while not binding it too strongly. For this reason, the cofactor is free inside the pores and can reach the active center of the enzyme. In **Table 12**, the immobilization and the activities of low concentrated (0.1 mg/g) NOX immobilized fast and slow are summarized.

Table 12 Activity and Immobilization of 0.1 mg/g immobilized NOX on PU-Gx-PEI with different spatial distributions. *Heterogeneous (Entry 1 and 2) and homogeneous (Entry 3 and 4) distributed NOX on PU-Gx-PEI are compared in their catalytic properties. The suspension of the solutions was 1:5 for the orbital shaking and 1:10 for magnetic stirring. The soluble enzyme had a specific activity of 14.11 U/mg under orbital shaking and 12.31 U/mg under magnetic stirring.*

Entry	Mixing Mode	Immo-bilization Yield (%)	Specific Activity (U/mg)	Expressed Activity ($U/g_{carrier}$)	Relative Recovered Activity (%)
1	Orbital Shaking	99.75 ± 0.00	**1.23 ± 0.19**	0.12 ± 0.02	8.70 ± 1.36
2	Magnetic Stirring		**6.07 ± 1.37**	0.61 ± 0.14	49.31 ± 11.16
3	Orbital Shaking	97.49 ± 0.10	**0.81 ± 0.45**	0.08 ± 0.05	5.77 ± 3.22
4	Magnetic Stirring		**2.16 ± 0.55**	0.35 ± 0.07	17.55 ± 4.44

The fast immobilized NOX exhibited a higher specific activity and a higher relative recovered activity. In agreement with previous results, magnetic stirring improves the catalytic performance of NOX. The influence of the spatial distribution of NOX immobilized on PU-Gx with and without PEI25 coating are depicted in **Figure 15**.

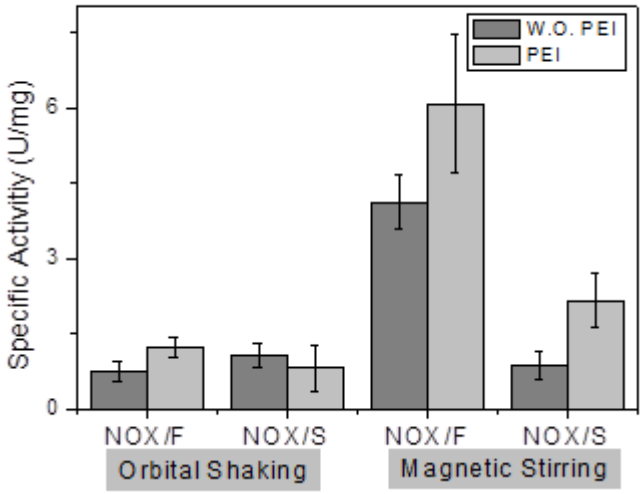

Figure 15 Influence of PEI coating on NOX immobilized on PU-Gx. *The homogeneous samples (NOX/S) are immobilized slowly by using 10 mM hydroxylamine and 30% (v/v) ethanol. The heterogeneous samples (NOX/F) do not have additives in the immobilization mixture. The dark grey bars represent the carrier without coating, the specific activities are shown in* ***Table 6****, and the light grey bars represent the carrier with PEI25 coating (****Table 12****).*

Generally, the PEI-coated carriers seemed to exhibited higher specific activities than non-coated carriers. However, the differences of the specific activities measured under orbital shaking conditions are not significant (**Figure 15**). As expected, the heterogeneous immobilized NOX exhibited higher specific activities. Under magnetic stirring condition the specific activity of the different enzyme preparations was increased. Both distributions, heterogeneous (NOX/F) and homogeneous (NOX/S), tend to exhibit higher catalytic performance when coated with PEI and under magnetic stirring conditions.

To sum up, 0.1 mg/g F demonstrated that a poor mixing and the lack of PEI-coating lead to lowest measured NOX activity, 0.75 U/mg. By changing the mixing method and additional PEI-coating, the specific activity increased about 8 fold and exhibited a specific activity of 6.07 U/mg. This example highlights the importance of aeration and the decrease of mass transfer limitations of cofactors in the reaction of NOX.

3.4.5 Determination of K_m

Previously, the K_m of NOX immobilized on AG-Gx has been determined as 2.1 mM NADH using 50 µM of FAD at 25°C and pH 7 [33]. The experiments presented throughout this thesis focused on the different distributions of NOX on the carrier and the enhancement of the cofactor accessibility by PEI coating. Therefore, K_m values of all immobilized preparations were determined. In all experiments, 1 mg/g NOX were

immobilized on AG-Gx and 0.15 mM of FAD (three times more than the concentration used by Rocha-Martín *et al.* [33]) was used to determine the Km of the immobilized enzymes towards NADH. **Figure 16** shows the Michaelis-Menten curves of 4 different preparations, heterogeneous (Fast) immobilized NOX on AG-Gx with and without PEI coating and homogenous (Slow) immobilized NOX on AG-Gx with and without PEI coating.

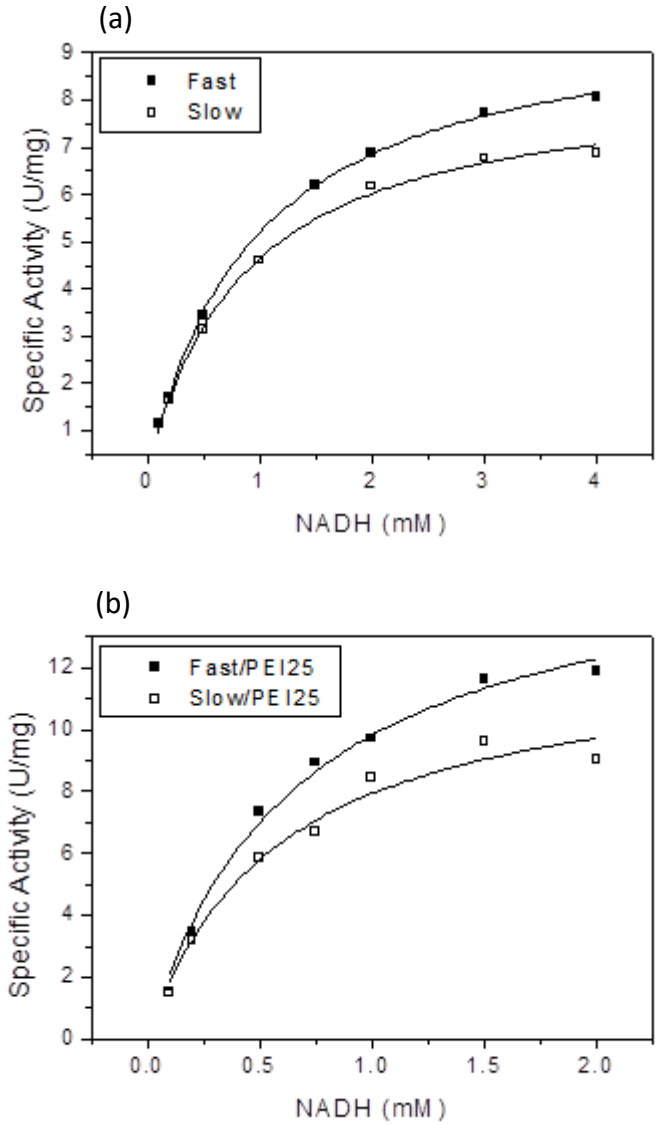

Figure 16 Determination of K_m of NOX immobilized on AG-Gx. *The samples were immobilized in 4 different variations: fast and slow (a) and fast and slow with PEI25-coating (b). "Fast" stands for the heterogeneous distribution (black boxes) and "Slow" is the equivalent to homogeneous distribution (white boxes). The reaction was done at 25°C and pH7 using 0.15 mM FAD.*

The reactions of the samples without PEI25-coating were conducted adding increasing concentrations of NADH up to 4 mM. However, a plateau was reached after 2 mM of NADH by employing PEI into the system. The uncoated as well as the PEI25-coated

biocatalyst showed similar behaviors. In contrast, the slow immobilized NOX exhibited a lower V_{max}. This indicates that the specific activity is limited by the mass transfer of the cofactor into the carrier depending on the distribution. **Table 13** summarizes the obtained K_m and V_{max}.

Table 13 K_m and V_{max} of fast, slow and fast and slow with PEI coating immobilized NOX. *1 mg/g NOX were immobilized and 0.15 mM FAD were used. The R2 was in all cases above 0.9. Vmax and Km of the different samples are shown as followed: Entry 1 fast immobilized NOX, Entry 2 slow immobilized NOX, Entry 3 fast immobilized NOX coated with PEI25, Entry 4 slow immobilized NOX coated with PEI25.*

Entry	Preparation	V_{max} (U/mg)	K_m (mM)
1	Fast	10.03 ± 0.16	0.93 ± 0.05
2	Slow	8.52 ± 0.20	0.83 ± 0.06
3	Fast PEI25	16.40 ± 0.94	0.67 ± 0.10
4	Slow PEI25	12.55 ± 0.99	0.58 ± 0.12

The PEI has a positive effect on the K_m and V_{max} (**Figure 16** and **Table 13**). The V_{max} increases 1.5 times and the K_m decreases 1.3 times. This supports the previous results that the PEI coating enhances the activity of immobilized NOX. The ratios of V_{max} and K_m between both distributions are similar to those of the samples with PEI-coating. This indicates that the PEI-coating marginally affects the mass transport of cofactor into the carrier with homogenous immobilized NOX. So far, the NADH consumption was monitored to detect the specific activity of NOX. To complement the characterization, the product formation is detected by implementing a bi-enzymatic system.

3.5 Bi-enzymatic system of NOX-HRP

HRP can oxidize H_2O_2 and reduce Ampliflu™ Red producing resorufin. The absorbance of the product resorufin is measured at 560 nm. This system poses an additional option to monitor the activity of NOX [60], [61]. In fact, this strategy allows for the monitoring of NADH and H_2O_2 simultaneously.

3.5.1 Co-enzymatic reaction of immobilized NOX and soluble HRP

The bi-enzymatic system was tested with 1 mg/g immobilized NOX on AG-Gx and soluble HRP. As described above, Ampliflu™ Red is used as the substrate of HRP.

The reaction catalyzed by HRP is dependent on the concentration of H_2O_2 formed by NOX [51], [60], [61]. Hence, the activity of HRP is a proxy for the activity of NOX.

Six different preparations of NOX were tested in order to incorporate every aspect of the possible parameters. Samples of immobilized NOX were prepared in a fast and slow manner on AG-Gx without additives (“classic”), with PEI25 added (“PEI25”) and with co-immobilized NADH (“PEI25 + NADH”). The observed catalytic performances are presented in **Figure 17**.

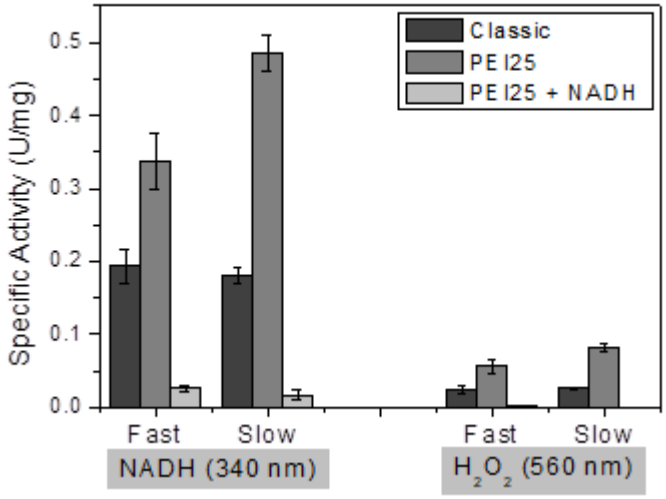

Figure 17 Specific activities of NOX on AG-Gx. The specific activity is measured and represented in two ways. *From left to right the specific examples are shown as followed: NADH consumption of fast and slow immobilized NOX (NADH) followed by the reaction of HRP with AmplifluTM Red of fast and slow immobilized NOX (H2O2). Samples of both measurements are depicted as followed: immobilized NOX "classic", immobilizations coated with PEI25 (PEI25) and immobilized NOX with co-immobilized NADH (PEI25 + NADH).*

The activity ratios between the reactions measured by NADH-consumption and the Ampliflu™ Red reaction are comparable (**Figure 17**). Nevertheless, the specific activity measured by HRP is about 6 to 7 times lower than the specific activity measured by NADH consumption.

The specific activities are summarized in **Table 14**.

Table 14 Specific activity of NOX measured by observing NADH-consumption at 340 nm (NOX - NADH) and by Ampliflu™ Red at 560 nm (HRP – H_2O_2). *NOX was immobilized slow and fast (classic), PEI25 indicates that the carrier was coated with PEI25 and PEI25 + NADH is the carrier with NOX and NADH immobilized. PEI25 + NADH has no soluble NADH in the reaction solution added. The suspension of the immobilized NOX and the reaction solution was 1:10. Specific activities are depicted as followed: Entry 1 shows the activity of heterogeneous immobilized NOX observed by NADH consumption, Entry 2 shows the activity of homogeneous immobilized NOX observed by NADH consumption, Entry 3 shows the activity of heterogeneous immobilized NOX observed by H2O2 production and Entry 4 shows the activity of homogeneous immobilized NOX observed by H2O2 production.*

Entry	Classic	PEI25	PEI25 + NADH
1	0.19 ± 0.02	0.34 ± 0.04	0.03 ± 0.01
2	0.18 ± 0.01	0.49 ± 0.02	0.02 ± 0.01
3	0.02 ± 0.01	0.06 ± 0.01	0.000 ± 0.00
4	0.03 ± 0.00	0.08 ± 0.00	0.00 ± 0.00

The lower activities obtained by HRP indicate that there might be mass transfer issues of NAD^+ which limit the reaction of soluble HRP. Another reason could be the HRP concentration in the reaction as HRP should not be fully saturated to show the real product formation of NOX. The product (H_2O_2) has to be transported from the carrier to the HRP in the bulk solution which results in a reaction rate limitation. Furthermore, it has to be considered that HRP might be inhibited by NADH. NADH is able to react with HRP and competes with Ampliflu™ Red as a substrate [62].

As NADH is consumed by NOX, the inhibition is mitigated and HRP can catalyze the reaction with Ampliflu™ Red. Both effects may well be a reason for the lower specific activity shown by HRP. Nonetheless, the ratios of the specific activities between “Classic” and “PEI25” in all cases were similar to the specific activities obtained by monitoring NADH consumption. This indicates that the specific activity monitored by substrate consumption is relatable to the product formation.

Moreover, the graphs in **Figure 17** show the increase of specific activity by coating the carrier with PEI25. As discussed in section 4, the PEI coating increases the catalytic performance by its ability to reversibly bind to the cofactors. In this experiment, we could show that the ratio of NADH and HRP observation is similar. Regardless which component is observed, substrate consumption or product formation, PEI increases the activity of NOX and mitigates the diffusion of the cofactor to the immobilized enzyme.

4 Conclusion

To conclude, we studied immobilized NOX on two different carriers, AG-Gx and PU-Gx. Therefore, we studied the spatial distribution of NOX on PU-GX, investigated the mass transfer limitations of substrate and cofactor and discussed the different properties of the carrier.

As previously shown, the use 10 mM of hydroxylamine promotes a homogeneous distribution of NOX onto AG-Gx [44]. PU-Gx has different material properties and we could show that neither hydroxylamine nor ethanolamine promote this effect of controlled distribution onto the carrier sufficient enough. Whereas, we could achieve a homogenous distributed NOX on PU-Gx using a combination of 30% ethanol and 10 mM hydroxylamine during the immobilization process. This is proven by the slow-down of the immobilization process as well as in the microscopy images.

It is well known that vigorous mixing improves overall suspension of the carrier in the solution and thus facilitate also the mass transfer [18]. We compared two different mixing modes to gain a better insight into mass transfer limitations. In all cases, the more vigorous mixing mode, magnetic stirring, leads to overall higher specific activities of immobilized NOX rather than the weaker, orbital shaking. This might correlate with a better mass transfer of oxygen as well as cofactors. Further, we could show that AG-Gx provide an even higher activity of NOX under magnetic stirring. This might be explained by the material properties. As mentioned above, AG-Gx is more hydrophilic rather than PU-Gx. This not only leads to a different immobilization behavior but also to a different mass transfer. The vigorous mixing might improve the mass transfer to the hydrophilic AG-Gx even more. Another interesting finding is that the higher enzyme loading has a lower specific activity compared to the lower enzyme loading. The observation of oxygen consumption allowed having a better understanding of the substrate limitations. Further on, we could demonstrate that the specific activity of NOX increases with increasing NADH concentration, which means that NADH limits the reaction.

To overcome mass transfer limitations of cofactors, we introduced PEI additionally onto the carrier. PEI binds reversibly NADH and FAD and facilitates cofactor accessibility for the enzyme. Therefore, we tested PEI-coatings with different molecular weights. We could show that the K_d of the PEI with the highest molecular weight (PEI10^6) is the

lowest which correlates with a better binding facility. Nonetheless, we want to achieve a better cofactor accessibility for which a PEI coating with lower molecular weight is more appropriate than the cofactor is more likely to lixiviate from the PEI. Therefore, several experiments were conducted using a PEI25- or PEI60-coating. Overall, we could once more show that magnetic stirring achieves a higher specific activity compared to orbital shaking. Reasons for this may be an enhanced mass transfer through vigorous mixing and a better surface aeration. Further on, NOX was able to achieve higher catalytic performances by introducing PEI on the carrier. The mass transfer limitations of cofactor are overcome for orbital shaking as well as magnetic stirring. By enhancing mixing and the incorporation of PEI, the mass transfer of cofactors as well as oxygen could be enhanced as shown in **Figure 15**. There, NOX immobilized on PU-Gx-PEI25 showed the highest specific activities of 6.07 U/mg under magnetic stirring rather than the ones of NOX without PEI coating (orbital shaking and magnetic stirring).

Generally, homogeneous distributed NOX shows weaker activity compared to the heterogeneous immobilizations. Even though the introduction of a PEI-coating enhances the catalytic properties, the heterogeneous catalyst shows higher specific activities. Further, the determination of K_m shows that the introduction barley enhances the mass transfer of cofactors.

To sum up, magnetic stirring provides optimal distribution of the carrier in the suspension and enhances mass transfer as well as surface aeration. The heterogeneous immobilized NOX shows in all cases better results rather than homogeneous distributions. Even the enhanced cofactor mass transfer by incorporation of PEI influences the catalytic properties marginally. Nevertheless, the heterogeneous immobilized NOX benefits from the PEI-coating and achieves the highest catalytic results using vigorous mixing.

As a future perspective, this work provides an enhanced understanding of immobilized NOX and mass transfer limitations were evaluated. As a next step, it can be considered to incorporate NOX into bi- or multi-enzymatic reactions. This could provide a basic understanding about the future incorporation of NOX as a cofactor recycling system.

5 References:

[1] J. Chapman, A. E. Ismail, and C. Z. Dinu, 'Industrial Applications of Enzymes: Recent Advances, Techniques, and Outlooks', *Catalysts*, vol. 8, no. 6, p. 238, Jun. 2018, doi: 10.3390/catal8060238.

[2] R. A. Sheldon and S. van Pelt, 'Enzyme immobilisation in biocatalysis: why, what and how', *Chem. Soc. Rev.*, vol. 42, no. 15, pp. 6223–6235, Jul. 2013, doi: 10.1039/C3CS60075K.

[3] U. Hanefeld, L. Gardossi, and E. Magner, 'Understanding enzyme immobilisation', *Chem. Soc. Rev.*, vol. 38, no. 2, pp. 453–468, Jan. 2009, doi: 10.1039/B711564B.

[4] C. Mateo, J. M. Palomo, G. Fernandez-Lorente, J. M. Guisan, and R. Fernandez-Lafuente, 'Improvement of enzyme activity, stability and selectivity via immobilization techniques', *Enzyme and Microbial Technology*, vol. 40, no. 6, pp. 1451–1463, May 2007, doi: 10.1016/j.enzmictec.2007.01.018.

[5] R. A. Sheldon, 'Enzyme Immobilization: The Quest for Optimum Performance', *Advanced Synthesis & Catalysis*, vol. 349, no. 8–9, pp. 1289–1307, 2007, doi: 10.1002/adsc.200700082.

[6] R. M. Lindeque, 'Reactor Selection for Effective Continuous Biocatalytic Production of Pharmaceuticals', *Catalysts*, vol. 9, no. 3, 2019, doi: 10.3390/catal9030262.

[7] A. C. Pierre, 'The Sol–Gel Encapsulation of Enzymes', *Biocatalysis and Biotransformation*, vol. 22, pp. 145–170, Jul. 2009, doi: 10.1080/10242420412331283314.

[8] J. Jegan Roy and T. Emilia Abraham, 'Strategies in Making Cross-Linked Enzyme Crystals', *Chem. Rev.*, vol. 104, no. 9, pp. 3705–3722, Sep. 2004, doi: 10.1021/cr0204707.

[9] R. A. Sheldon, 'Characteristic features and biotechnological applications of cross-linked enzyme aggregates (CLEAs)', *Appl Microbiol Biotechnol*, vol. 92, no. 3, pp. 467–477, Nov. 2011, doi: 10.1007/s00253-011-3554-2.

[10] N. R. Mohamad, N. H. C. Marzuki, N. A. Buang, F. Huyop, and R. A. Wahab, 'An overview of technologies for immobilization of enzymes and surface analysis techniques for immobilized enzymes', *Biotechnol Biotechnol Equip*, vol. 29, no. 2, pp. 205–220, Mar. 2015, doi: 10.1080/13102818.2015.1008192.

[11] E. Katchalski-Katzir and D. M. Kraemer, 'Eupergit® C, a carrier for immobilization of enzymes of industrial potential', *Journal of Molecular Catalysis B: Enzymatic*, vol. 10, no. 1, pp. 157–176, Oct. 2000, doi: 10.1016/S1381-1177(00)00124-7.

[12] B. Krajewska, 'Application of chitin- and chitosan-based materials for enzyme immobilizations: a review', *Enzyme and Microbial Technology*, vol. 35, no. 2, pp. 126–139, Aug. 2004, doi: 10.1016/j.enzmictec.2003.12.013.

[13] B. Brena, P. González-Pombo, and F. Batista-Viera, 'Immobilization of enzymes: a literature survey', *Methods Mol. Biol.*, vol. 1051, pp. 15–31, 2013, doi: 10.1007/978-1-62703-550-7_2.

[14] V. Grazú, O. Abian, C. Mateo, F. Batista-Viera, R. Fernández-Lafuente, and J. M. Guisán, 'Stabilization of enzymes by multipoint immobilization of thiolated proteins on new epoxy-thiol supports', *Biotechnology and Bioengineering*, vol. 90, no. 5, pp. 597–605, 2005, doi: 10.1002/bit.20452.

[15] F. López-Gallego, G. Fernández-Lorente, J. Rocha Martín, J. Bolivar, C. Mateo, and J. Guisan, 'Stabilization of Enzymes by Multipoint Covalent Immobilization on Supports Activated with Glyoxyl Groups', in *Methods in molecular biology (Clifton, N.J.)*, vol. 1051, 2013, pp. 59–71.

[16] F. López-Gallego, J. Guisan, and L. Betancor, 'Glutaraldehyde-Mediated Protein Immobilization', *Methods in molecular biology (Clifton, N.J.)*, vol. 1051, pp. 33–41, Aug. 2013, doi: 10.1007/978-1-62703-550-7_3.

[17] C. Mateo, V. Grazu, J. M. Palomo, F. López-Gallego, R. Fernandez-Lafuente, and J. Guisan, 'Immobilization of enzymes on heterofunctional epoxy supports', *Nature protocols*, vol. 2, pp. 1022–33, Feb. 2007, doi: 10.1038/nprot.2007.133.

[18] P. M. Doran, *Bioprocess Engineering Principles*, 2nd ed. Academic Press, 2013.

[19] S. Andreescu, B. Bucur, and J.-L. Marty, 'Affinity Immobilization of Tagged Enzymes', in *Immobilization of Enzymes and Cells*, J. M. Guisan, Ed. Totowa, NJ: Humana Press, 2006, pp. 97–106.
[20] A. Liese and L. Hilterhaus, 'Evaluation of immobilized enzymes for industrial applications', *Chem. Soc. Rev.*, vol. 42, no. 15, pp. 6236–6249, Jul. 2013, doi: 10.1039/C3CS35511J.
[21] J. M. Bolivar and B. Nidetzky, 'The Microenvironment in Immobilized Enzymes: Methods of Characterization and Its Role in Determining Enzyme Performance', *Molecules*, vol. 24, no. 19, Sep. 2019, doi: 10.3390/molecules24193460.
[22] J. L. V. Roon, M. Joerink, M. P. W. M. Rijkers, J. Tramper, C. G. P. H. Schroën, and H. H. Beeftink, 'Enzyme Distribution Derived from Macroscopic Particle Behavior of an Industrial Immobilized Penicillin-G Acylase', *Biotechnology Progress*, vol. 19, no. 5, pp. 1510–1518, 2003, doi: 10.1021/bp0340638.
[23] Md. M. Hossain and D. D. Do, 'Effects of nonuniform immobilized enzyme distribution in porous solid supports on the performance of a continuous reactor', *The Chemical Engineering Journal*, vol. 34, no. 2, pp. B35–B47, Feb. 1987, doi: 10.1016/0300-9467(87)87011-9.
[24] K. E. Dennis, D. S. Clark, J. E. Bailey, Y. K. Cho, and Y. H. Park, 'Immobilization of enzymes in porous supports: Effects of support–enzyme solution contacting', *Biotechnology and Bioengineering*, vol. 26, no. 8, pp. 892–900, 1984, doi: 10.1002/bit.260260812.
[25] J. M. Bolivar, T. Consolati, T. Mayr, and B. Nidetzky, 'Shine a light on immobilized enzymes: real-time sensing in solid supported biocatalysts', *Trends in Biotechnology*, vol. 31, no. 3, pp. 194–203, Mar. 2013, doi: 10.1016/j.tibtech.2013.01.004.
[26] J. M. Bolivar, I. Eisl, and B. Nidetzky, 'Advanced characterization of immobilized enzymes as heterogeneous biocatalysts', *Catalysis Today*, vol. 259, pp. 66–80, Jan. 2016, doi: 10.1016/j.cattod.2015.05.004.
[27] Y. Zhang and H. Hess, 'Toward Rational Design of High-efficiency Enzyme Cascades', *ACS Catal.*, vol. 7, no. 9, pp. 6018–6027, Sep. 2017, doi: 10.1021/acscatal.7b01766.
[28] C. Schmid-Dannert and F. López-Gallego, 'Advances and opportunities for the design of self-sufficient and spatially organized cell-free biocatalytic systems', *Current Opinion in Chemical Biology*, vol. 49, pp. 97–104, Apr. 2019, doi: 10.1016/j.cbpa.2018.11.021.
[29] J. Rocha-Martín, B. de las Rivas, R. Muñoz, J. M. Guisán, and F. López-Gallego, 'Rational Co-Immobilization of Bi-Enzyme Cascades on Porous Supports and their Applications in Bio-Redox Reactions with In Situ Recycling of Soluble Cofactors', *ChemCatChem*, vol. 4, no. 9, pp. 1279–1288, Sep. 2012, doi: 10.1002/cctc.201200146.
[30] W. A. van der Donk and H. Zhao, 'Recent developments in pyridine nucleotide regeneration', *Current Opinion in Biotechnology*, vol. 14, no. 4, pp. 421–426, Aug. 2003, doi: 10.1016/S0958-1669(03)00094-6.
[31] R. Cutlan, S. De Rose, M. N. Isupov, J. A. Littlechild, and N. J. Harmer, 'Using enzyme cascades in biocatalysis: Highlight on transaminases and carboxylic acid reductases', *Biochimica et Biophysica Acta (BBA) - Proteins and Proteomics*, vol. 1868, no. 2, p. 140322, Feb. 2020, doi: 10.1016/j.bbapap.2019.140322.
[32] Q. Ji, B. Wang, J. Tan, L. Zhu, and L. Li, 'Immobilized multienzymatic systems for catalysis of cascade reactions', *Process Biochemistry*, vol. 51, no. 9, pp. 1193–1203, Sep. 2016, doi: 10.1016/j.procbio.2016.06.004.
[33] J. Rocha-Martín *et al.*, 'New biotechnological perspectives of a NADH oxidase variant from Thermus thermophilus HB27 as NAD+-recycling enzyme', *BMC Biotechnol*, vol. 11, p. 101, Nov. 2011, doi: 10.1186/1472-6750-11-101.
[34] Y. Nishiyama *et al.*, 'Hydrogen Peroxide-Forming NADH Oxidase Belonging to the Peroxiredoxin Oxidoreductase Family: Existence and Physiological Role in Bacteria', *J Bacteriol*, vol. 183, no. 8, pp. 2431–2438, Apr. 2001, doi: 10.1128/JB.183.8.2431-2438.2001.
[35] Phillip R. Gibbs, Andreas S. Bommarius, and Bettina R. Riebel, 'Cofactor Regeneration of NAD+ from NADH: Novel Water-Forming NADH Oxidases'. Wiley-VCH Verlag GmbH & Co. KGaA, Aug. 2002, Accessed: Mar. 17, 2019. [Online]. Available:

https://onlinelibrary.wiley.com/doi/epdf/10.1002/1615-4169%28200212%29344%3A10%3C1156%3A%3AAID-ADSC1156%3E3.0.CO%3B2-%23.
[36] J. R. Hillebrecht, K. J. Wise, J. F. Koscielecki, and R. R. Birge, 'Directed Evolution of Bacteriorhodopsin for Device Applications', in *Methods in Enzymology*, vol. 388, Academic Press, 2004, pp. 333–347.
[37] J. Rocha-Martin, P. A. Sánchez-Murcia, F. López-Gallego, A. Hidalgo, J. Berenguer, and J. M. Guisan, 'Functional Characterization and Structural Analysis of NADH Oxidase Mutants from Thermus thermophilus HB27: Role of Residues 166, 174, and 194 in the Catalytic Properties and Thermostability', *Microorganisms*, vol. 7, no. 11, Art. no. 11, Nov. 2019, doi: 10.3390/microorganisms7110515.
[38] C. A. Hone and C. O. Kappe, 'The Use of Molecular Oxygen for Liquid Phase Aerobic Oxidations in Continuous Flow', *Top Curr Chem (Cham)*, vol. 377, no. 1, 2019, doi: 10.1007/s41061-018-0226-z.
[39] J. M. Bolivar, A. Mannsberger, M. S. Thomsen, G. Tekautz, and B. Nidetzky, 'Process intensification for O2-dependent enzymatic transformations in continuous single-phase pressurized flow', *Biotechnol Bioeng*, vol. 116, no. 3, pp. 503–514, Mar. 2019, doi: 10.1002/bit.26886.
[40] J. Wiesbauer, M. Cardinale, and B. Nidetzky, 'Shaking and stirring: Comparison of controlled laboratory stress conditions applied to the human growth hormone', *Process Biochemistry*, vol. 48, no. 1, pp. 33–40, Jan. 2013, doi: 10.1016/j.procbio.2012.11.007.
[41] J. G. Biddlecombe *et al.*, 'Factors influencing antibody stability at solid–liquid interfaces in a high shear environment', *Biotechnology Progress*, vol. 25, no. 5, pp. 1499–1507, 2009, doi: 10.1002/btpr.211.
[42] W. V. Hecke *et al.*, 'Bubble-free oxygenation of a bi-enzymatic system: effect on biocatalyst stability', *Biotechnology and Bioengineering*, vol. 102, no. 1, pp. 122–131, 2009, doi: 10.1002/bit.22042.
[43] J. M. Bolivar, T. Consolati, T. Mayr, and B. Nidetzky, 'Quantitating intraparticle O2 gradients in solid supported enzyme immobilizates: Experimental determination of their role in limiting the catalytic effectiveness of immobilized glucose oxidase', *Biotechnology and Bioengineering*, vol. 110, no. 8, pp. 2086–2095, Aug. 2013, doi: 10.1002/bit.24873.
[44] A. I. Benítez-Mateos, 'Design and engineering of artificial metabolic cells for chemical manufacturing.', Apr. 2019, doi: http://hdl.handle.net/10810/33126.
[45] Y. Koyama, T. Hoshino, N. Tomizuka, and K. Furukawa, 'Genetic transformation of the extreme thermophile Thermus thermophilus and of other Thermus spp.', *J Bacteriol*, vol. 166, no. 1, pp. 338–340, Apr. 1986.
[46] '4x Laemmli Sample Buffer #1610747 | Life Science Research | Bio-Rad'. https://www.bio-rad.com/de-at/sku/1610747-4x-laemmli-sample-buffer?ID=1610747 (accessed Jul. 15, 2020).
[47] 'Coomassie', *Protocols Online*, Apr. 01, 2012. https://www.protocolsonline.com/protein-science/coomassie/ (accessed Oct. 14, 2019).
[48] 'Quick Start™ Bradford Protein Assay | Life Science Research | Bio-Rad'. https://www.bio-rad.com/de-at/product/quick-start-bradford-protein-assay?ID=5ec149ee-0cd1-468b-8651-a2fe9de6944d (accessed Jul. 15, 2020).
[49] M. M. Bradford, 'A rapid and sensitive method for the quantitation of microgram quantities of protein utilizing the principle of protein-dye binding', *Analytical Biochemistry*, vol. 72, no. 1, pp. 248–254, May 1976, doi: 10.1016/0003-2697(76)90527-3.
[50] 'Bio-Rad Protein Assay | Life Science Research | Bio-Rad'. https://www.bio-rad.com/de-at/product/bio-rad-protein-assay?ID=d4d4169a-12e8-4819-8b3e-ccab019c6e13 (accessed Oct. 04, 2019).
[51] 'Using Ampliflu™ Red Substrate for fluorescence-based Western Blotting', *Sigma-Aldrich*. https://www.sigmaaldrich.com/technical-documents/articles/biology/ampliflu-red-fluorescence-substrate-for-western-blotting.html (accessed Sep. 24, 2019).

[52] JoséM. Guisán, 'Aldehyde-agarose gels as activated supports for immobilization-stabilization of enzymes', *Enzyme and Microbial Technology*, vol. 10, no. 6, pp. 375–382, Jun. 1988, doi: 10.1016/0141-0229(88)90018-X.
[53] C. Mateo *et al.*, 'Improvement of Enzyme Properties with a Two-Step Immobilizaton Process on Novel Heterofunctional Supports', *Biomacromolecules*, vol. 11, no. 11, pp. 3112–3117, Nov. 2010, doi: 10.1021/bm100916r.
[54] P. L. Sciences, 'Purolite Life Science Product: Lifetech™ ECR8204F'. http://www.purolite.com/ls-product/ecr8204f (accessed Oct. 21, 2019).
[55] O. Barbosa, R. Torres, C. Ortiz, and R. Fernandez-Lafuente, 'The slow-down of the CALB immobilization rate permits to control the inter and intra molecular modification produced by glutaraldehyde', *Process Biochemistry*, vol. 47, no. 5, pp. 766–774, May 2012, doi: 10.1016/j.procbio.2012.02.009.
[56] S. Velasco-Lozano, A. I. Benítez-Mateos, and F. López-Gallego, 'Co-immobilized Phosphorylated Cofactors and Enzymes as Self-Sufficient Heterogeneous Biocatalysts for Chemical Processes', *Angew Chem Int Ed Engl*, vol. 56, no. 3, pp. 771–775, Jan. 2017, doi: 10.1002/anie.201609758.
[57] K. H. Chu and M. A. Hashim, 'Protein adsorption on Ion exchange resin: Estimation of equilibrium isotherm parameters from batch kinetic data', *Biotechnol. Bioprocess Eng.*, vol. 11, no. 1, pp. 61–66, Feb. 2006, doi: 10.1007/BF02931870.
[58] J. Rocha-Martín, B. de las Rivas, R. Muñoz, J. M. Guisán, and F. López-Gallego, 'Rational Co-Immobilization of Bi-Enzyme Cascades on Porous Supports and their Applications in Bio-Redox Reactions with In Situ Recycling of Soluble Cofactors', *ChemCatChem*, vol. 4, no. 9, pp. 1279–1288, 2012, doi: 10.1002/cctc.201200146.
[59] M.-O. Månsson and K. Mosbach, '[1] Immobilized active coenzymes', in *Methods in Enzymology*, vol. 136, Academic Press, 1987, pp. 3–9.
[60] F. A. Summers, B. Zhao, D. Ganini, and R. P. Mason, 'Chapter One - Photooxidation of Amplex Red to Resorufin: Implications of Exposing the Amplex Red Assay to Light', in *Methods in Enzymology*, vol. 526, E. Cadenas and L. Packer, Eds. Academic Press, 2013, pp. 1–17.
[61] M. Zhou, Z. Diwu, N. Panchuk-Voloshina, and R. P. Haugland, 'A Stable Nonfluorescent Derivative of Resorufin for the Fluorometric Determination of Trace Hydrogen Peroxide: Applications in Detecting the Activity of Phagocyte NADPH Oxidase and Other Oxidases', *Analytical Biochemistry*, vol. 253, no. 2, pp. 162–168, Nov. 1997, doi: 10.1006/abio.1997.2391.
[62] L. A. Marquez and H. B. Dunford, 'Transient and Steady-State Kinetics of the Oxidation of Scopoletin by Horseradish Peroxidase Compounds I, II and III in the Presence of NADH', *European Journal of Biochemistry*, vol. 233, no. 1, pp. 364–371, 1995, doi: 10.1111/j.1432-1033.1995.364_1.x.